WIPP Library

ENTERED

EEG-21

The Geochemistry of Two Pressurized Brines From the Castile Formation in the Vicinity of the Waste Isolation Pilot Plant (WIPP) Site

Stuart Faith, M.S., P.E.
Peter Spiegler, Ph.D.
Kenneth R. Rehfeldt, M.S.

Environmental Evaluation Group
Environmental Improvement Division
Health and Environment Department
State of New Mexico

April 1983

830401

Environmental Evaluation Group
Reports

EEG-1 Goad, Donna. A Compilation of Site Selection Criteria, Considerations and Concerns Appearing in the Literature on the Deep Disposal of Radioactive Wastes, June 1979.

EEG-2 Review Comments on Geological Characterization Report, Waste Isolation Pilot Plant (WIPP) Site, Southeastern New Mexico SAND 78-1596, Volumes I and II, December 1978.

EEG-3 Neill, Robert H., et al, eds. Radiological Health Review of the Draft Environmental Impact Statement (DOE/EIS-0026-D) Waste Isolation Pilot Plant, U. S. Department of Energy, August 1979.

EEG-4 Little, Marshall S. Review Comments on the Report of the Steering Committee on Waste Acceptance Criteria for the Waste Isolation Pilot Plant, February 1980.

EEG-5 Channell, James K. Calculated Radiation Doses From Deposition of Material Released in Hypothetical Transportation Accidents Involving WIPP-Related Radioactive Wastes, November 1980.

EEG-6 Geotechnical Considerations for Radiological Hazard Assessment of WIPP. A Report of a Meeting Held on January 17-18, 1980, April 1980.

EEG-7 Chaturvedi, Lokesh WIPP Site and Vicinity Geological Field Trip. A Report of a Field Trip to the Proposed Waste Isolation Pilot Plant Project in Southeastern New Mexico, June 16 to 18, 1980, November 1980.

EEG-8 Wofsy, Carla. The Significance of Certain Rustler Aquifer Parameters for Predicting Long-Term Radiation Doses From WIPP, September 1980.

EEG-9 Spiegler, Peter. An Approach to Calculating Upper Bounds on Maximum Individual Doses From the Use of Contaminated Well Water Following a WIPP Repository Breach, September 1981.

EEG-10 Radiological Health Review of the Final Environmental Impact Statement (DOE/EIS-0026) Waste Isolation Pilot Plant, U. S. Department of Energy, January 1981.

(Continued on back cover)

The Geochemistry of Two Pressurized Brines from the Castile Formation in the Vicinity of the Waste Isolation Pilot Plant (WIPP) Site

Environmental Evaluation Group
Environmental Improvement Division
Health and Environment Department
P.O. Box 968
Santa Fe, New Mexico

April 1983

CONTENTS

Title	Page
FOREWORD	i
STAFF AND CONSULTANTS	ii
SUMMARY	iii
1.0 INTRODUCTION	1
2.0 SAMPLE DATA	2
2.1 Statistical Treatment of Data	2
2.2 Limitations of t-statistic	5
3.0 ANALYSIS OF STATISTICAL DIFFERENCES	6
3.1 Sample Set Comparisons	6
3.1.1 Field Versus Laboratory Analysis of Flowed Samples	6
3.1.2 Flowed Versus Downhole Samples	8
3.1.3 Core Laboratory versus D'Appolonia laboratory	9
3.2 Differences Between ERDA-6 and WIPP-12	9
4.0 BRINE ISOTOPIC FRACTIONATIONS	16
4.1 Isotopic Thermometers	16
4.2 Isotope Fractionation Factors	17
4.3 Discussion	18
4.3.1 Oxygen Fractionation	18
4.3.2 Carbon Fractionation	19
4.3.3 Hydrogen (deuterium) Fractionation	19
5.0 URANIUM DISEQUILIBRIUM	23

5.1 Theoretical Considerations 23

5.2 Initial Conditions -- Set 1 25

5.2.1 Age Calculations 29
5.2.2 Discussion -- Initial Condition -- Set 1 30

5.3 Initial Condition -- Set 2 30

5.3.1 Age Calculations 31
5.3.2 Discussion -- Initial Condition -- Set 2 33

5.4 General Discussion of Uranium Disequilibrium 33

6.0 MAJOR AND MINOR ELEMENT CHEMISTRY 35

6.1 Equilibrium Thermodynamic Modeling 35

6.1.1 Background and Application 35
6.1.2 Limitations of Equilibrium Modeling 36
6.1.3 Results of Equilibrium Modeling 38

6.2 Major/Minor Brine Chemistry Interpretation 39

6.2.1 Bromide Ratios 39

7.0 CONCLUSIONS 49

8.0 RECOMMENDATIONS 50

REFERENCES 52

APPENDIX 56

Table 1: ERDA-6 & WIPP-12 Sample Statistical Groups 57
Table 2: T-Test Results 58
Table 3: Mean, Deviation and Number of Samples 62

FOREWORD

The purpose of the Environmental Evaluation Group (EEG) is to conduct an independent technical evaluation of the potential radiation exposure to people from the proposed Federal radioactive Waste Isolation Pilot Plant (WIPP) near Carlsbad, in order to protect the public health and safety and ensure that there is minimal environmental degradation. The EEG is part of the Environmental Improvement Division, a component of the New Mexico Health and Environment Department -- the agency charged with the primary responsibility for protecting the health of the citizens of New Mexico.

The Group is neither a proponent nor an opponent of WIPP.

Analyses are conducted of available data concerning the proposed site, the design of the repository, its planned operation, and its long-term stability. These analyses include assessments of reports issued by the U.S. Department of Energy (DOE) and its contractors, other Federal agencies and organizations, as they relate to the potential health, safety and environmental impacts from WIPP.

The project is funded entirely by the U.S. Department of Energy through Contract DE-AC04-79AL10752 with the New Mexico Health and Environment Department.

Robert H. Neill
Director

STAFF AND CONSULTANTS

James K. Channell, Ph.D., P.E., Environmental Engineer
Lokesh Chaturvedi, Ph.D., Engineering Geologist
Jo Anna De Carlo, Secretary
Stuart Faith, M.S., P.E., Consulting Geochemist
Luz Elena Garcia, B.B.E., Administrative Secretary
Marshall S. Little([1]), M.S., Health Physicist
Jack M. Mobley, B.A., Scientific Liaison Officer
Robert H. Neill, M.S., Director
Kenneth R. Rehfeldt, M.S., Hydrologist
Norma I. Silva, Administrative Officer
Peter Spiegler([1]) ([2]), Ph.D., Radiological Health Analyst
Robbe Tucker, M.L.S., Librarian

([1]) Certified, American Board of Health Physics
([2]) Certified, American College of Radiology

SUMMARY

The major and minor element data and isotopic data from the ERDA-6 and WIPP-12 testing indicate that the brine reservoirs encountered in the Upper Castile Formation are largely in equilibrium with their surrounding host rock environment. This contention is supported by thermodynamic and stable isotope data. It is not possible to assign an absolute age to the brine based on uranium disequilibrium considerations, but if the data is taken as an indicator of its age, then the brine has been a stagnant, chemically isolated body of fluid for no more than about two million years. Information and data evaluated herein indicate the likelihood that the brines encountered are predominantly, if not entirely, derived from a trapped seawater source subsequently modified by diagenesis. Major ion/bromide ratios indicate that halite dissolution has occurred to some extent subsequent to deposition of the Castile anhydrites and entrapment of the seawater brine. Mechanisms for additional halite dissolution are discussed. Based on the degree of present halite saturation, it is concluded that the potential for future dissolution of halite is minimal.

1.0 INTRODUCTION & PURPOSE

The origin of brines and coexisting gas and solid phases within the Upper Castile formation have been studied extensively during the period 1979 to the present by the U.S. Department of Energy, their technical and support contractors and independent review personnel. The potential effect of the pressurized Castile brine reservoirs on the WIPP geologic repository environment has been the subject of considerable debate and investigation.

The purpose of this report is to provide the New Mexico Environmental Evaluation Group's (EEG) analysis and summary comments concerning the geochemistry of two brine reservoirs in the Castile formation as they relate to the integrity of the proposed WIPP nuclear waste repository.

A considerable amount of investigative effort regarding these Castile brines has been conducted by Sandia National Laboratories and D'Appolonia Consulting Engineers. During the latter part of 1981, D'Appolonia Consultants performed extensive geologic, hydrologic and chemical evaluations of the ERDA-6 and WIPP-12 boreholes. In WIPP-12, pressurized brine was encountered in the upper anhydrite during deepening of the borehole. In ERDA-6, pressurized brine had previously been encountered in 1975 and reopened for study under the terms of a Stipulated Agreement between DOE and New Mexico. This report relies extensively on the chemical and isotope data collected from WIPP-12 and ERDA-6 and analyzed by D'Appolonia during the 1981/82 timeframe and presented in two separate reports, (ref. 1 and 2).

This report is divided into four sections which discuss:

(a) Sample data
(b) Statistical differences between sample data sets
(c) Brine isotopic fractionations
(d) Uranium disequilibrium
(e) Major/Minor Element chemistry
(f) Conclusions and recommendations

2.0 SAMPLE DATA

The brine data examined and discussed herein were taken predominantly from the Data File Report ERDA-6 and WIPP-12 Testing, Vols. I-V, prepared for Westinghouse Electric Corp. and U.S. Department of Energy by D'Appolonia, February, 1982. Additional analytical data were examined which were provided by the New Mexico Bureau of Mines and Mineral Resources for five samples collected from ERDA-6 and WIPP-12 and were found to be in general agreement with the more extensive D'Appolonia data. Some variations are noted for alkalinity between the NMBMMR and D'Appolonia data, which are attributed to precipitation of carbonates during sample holding times.

Analyses of data on brine from the Union and Shell Bootleg drill holes were also examined. (The location of these and other brine encounters is shown in Figure 6-11 of ref. 2). These additional data sets (NMBMMR, Union & Shell) were average values and were not sufficient to include in the statistical tests discussed subsequently. Additionally, the oxygen, deuterium, carbon and sulfur stable isotope and the uranium disequilibrium data were not analyzed for statistical deviations as were the major and minor chemical data. The reports by D'Appolonia (ref. 1 and 2) provide the most comprehensive documentation of sampling and analytical methodology which has been provided to date on the upper Castile, and are amenable to statistical analysis for purposes of determining natural versus sampling and/or analytically induced variability in brine data. Such determinations are a desirable prerequisite to interpretive analysis concerning fluid/reservoir genesis in the upper Castile brine reservoir(s).

2.1 Statistical Treatment of Data

During the testing conducted by D'Appolonia on the ERDA-6 and WIPP-12 boreholes, brine and gas samples from the upper Castile were collected for major, minor, trace and isotopic chemical analyses. The methods of sample collection may be broadly classified under the following two general headings:

(a) Brine samples were collected by allowing the well to flow under natural pressurization to the surface. Assuming that the brine flow

occurred from fracture zones in the upper anhydrite layer of the Castile, the brine samples contacted roughly 2000 vertical feet of Salado halite prior to their emergence through surface casing and appurtenant surface collection equipment. The samples were, at various times during any given flow test, analyzed for different chemical parameters in the field or stabilized and shipped to commercial laboratories for analysis, and

(b) Brine samples collected from isolated production zones in the upper anhydrite layer of the Castile by means of straddle packers and allowing the brine to flow through the drillstem or into sample containers to surface collection equipment. Downhole tests and samples were not allowed to coalesce with other formation fluids or minerals prior to their collection, and were stabilized and preserved in the field prior to shipment to analytical laboratories.

From the above general classification of sampling methodology, the samples may be divided into the following groups:

(a) flow test - field analyzed
(b) flow test - laboratory analyzed
(c) downhole - laboratory analyzed

The following statistical analyses were performed: Tables 1, 2 and 3 in the Appendix contain a tabulation of the inter and intra (i.e., among sample and within sample) groupings of statistical data. Table 1 shows the numerical identification of each sample group as well as combined groups of sample data. Table 3 provides mean, standard deviation and number of observations for various brine parameters for the ERDA-6 and WIPP-12 sample groups. Table 2 provides the t-statistic, the probability level of Type I errors associated with the null hypothesis ($\mu_1 = \mu_2$) and the degrees of freedom associated with each t-statistic. The methods used to calculate these statistics are given below:

Sample mean:

$$\overline{X}_i = \frac{\sum_{j=1}^{N_i} x_{ij}}{N_i}$$

Where: $\overline{X}_i$ = mean concentration of the $_i$th chemical parameter in units reported by D'Appolonia (eg. mg/ℓ)

N_i = number of samples for the particular sample grouping for which the $_i$th chemical parameter was measured.

Standard Deviation:

$$S_i = \frac{\sum_{j=1}^{N_i} (X_{ij} - \overline{X}_i)^2}{N_i}$$

S_i = standard deviation of the $_i$th chemical parameter in units

t-statistic:

$$t_i = \frac{\overline{X}_{1i} - \overline{X}_{2i}}{\sigma_i (1/N_{1i} + 1/N_{2i})^{1/2}}$$

Where: t_i = the student's t statistic for comparing two means (X_{1i} and X_{2i}) from sample group 1 and 2 for the $_i$th chemical parameter.

$N_{1,2i}$ = the number of samples in the sample group 1 and 2 for the $_i$th chemical parameter, and

$$\sigma_i = \left(\frac{N_{1i} S_{1i}^2 + N_{2i} S_{2i}^2}{N_{1i} + N_{2i} - 2} \right)^{1/2}$$

γ (degrees of freedom):

$\gamma = N_{1i} + N_{2i} - 3$

α probability:

Note: sample group notation of 1 and 2 may refer to any two separate sample population groups.

α = probability of error associated with rejecting the hypothesis: ($\mu_1 = \mu_2$) when in fact the hypothesis should be accepted as true (Type I error).

$$\alpha = \sin\left(1 + \frac{1}{2}\cos^2\theta + \frac{1\times3}{2\times4}\cos^4\theta + \ldots\frac{1\times3\times5\ldots(\gamma-3)}{3\times5\ldots(\gamma-2)}\cos^{\gamma-1}\theta\right)$$

for γ odd:

$$\alpha = \left[\frac{2}{\pi}\right]\left[\theta+\sin\theta\left(\cos\theta+\frac{2}{3}\cos^3\theta+\ldots\frac{2\times4\ldots(\gamma-3)}{3\times5\ldots(\gamma-2)}\cos^{\gamma-2}\theta\right)\right]$$

$$\text{and } \theta = \arctan\frac{t}{\sqrt{\gamma}}$$

For α values falling below an arbitrary value of 0.05 (5% probability level), it can be assumed that the two sample populations compared have statistically different concentration means for the particular chemical parameter considered.

2.2 Limitations of t-statistic

The Students t-test analysis, which is described above in Section 2.1 and is further discussed in Section 3.0, is but one technique that may be utilized to discern the discrete variabilities inherent in any set of sample populations. The t-test is strictly limited in its interpretation to determining if the mean of one sample population is statistically distinct from another sample population. The t-test is not a valid tool for interpreting the sources of sample population variability nor the distribution of sample population data. However, as a first order statistical tool, the t-test does allow one to verify the validity of assuming that the mean downhole chemical concentration is statistically equal or unequal to the flowed sample chemical concentration. These differences will be discussed more fully in Section 3.0.

3.0 ANALYSES OF STATISTICAL DIFFERENCES

In the case of the ERDA-6 and WIPP-12 major, minor and trace element data, the statistical differences between population means may be reviewed with the aid of Tables 2 and 3 in the Appendix. As was mentioned in Section 2.0, the brine chemical data may be broadly subdivided into categories of field versus laboratory sample groups, flowed versus downhole samples and finally ERDA-6 versus WIPP-12 samples. Within these three broad classifications of sample data there are numerous permutations or combinations of sample data which can be grouped individually or in sets for purposes of comparison and analysis. Obviously, all possible sample set and subset combinations do not need to be compared (e.g., WIPP-12; Flow test-2; field analyses have no significant meaning when compared to ERDA-6; downhole; laboratory tests). However, a number of comparisons of sample data are worthy of some examination.

The following Section 3.1 describes various sample data set combinations and their respective mean differences. The t-test and the respective probabilities of difference (see Section 2.1 for a brief discussion of the null hypothesis) relate only to the means or averages of the respectively compared sample population sets, and do not in and of themselves provide enough statistical information to infer the degree of variability attributable to sampling, analytical or natural variability. They do, however, suggest possible mechanisms of variance, which may be operative on the different sample sets.

3.1 Sample Set Comparisons

The following subsections discuss the differences between individual sample sets and combinations of sample sets as shown in Tables 1 through 3.

3.1.1 Field versus laboratory analysis of flowed samples.

As noted by D'Appolonia regarding sampling, there are relatively greater numbers of samples, which were analyzed in the field for various chemical

parameters than in the case of laboratory samples, for which there are fewer samples and a greater number of chemical parameters analyzed. This was necessary to provide a rapid method, while in the field, of determining the extent to which the changes in chemical composition with respect to time and volume of flowed sample had stabilized so that representative samples for detailed laboratory chemical analyses could be collected. The analysis of statistical reliability in the chemical results between field collection and laboratory determinations is limited to those chemical parameters which were analyzed at both locations.

From Tables 1 and 2, the following mean (average) concentrations are statistically different between field and laboratory for:

(a) chloride in ERDA-6; Flow Test-2
(b) specific conductance, chloride and sulfate for ERDA-6; Flow Test-3
(c) pH, chloride and sulfate for WIPP-12; Flow Test-1
(d) pH, specific conductivity and bicarbonate for WIPP-12; Flow Test-3

Suggested mechanisms or causes of these shifts are noted below.

(a) Since Chloride is not sufficiently reactive to change its liquid concentration after exposure to air or other sample contaminant sources, the difference between laboratory and field results may be attributable to differences in analytical procedures.

(b) Sulfate usually results from oxidation of more reduced sulfide species (H_2S, HS^-, S^{-2}). Therefor, the differences in sulfate concentrations between field and laboratory analyses may be caused by variation in the oxidation of the sulfide species H_2S, HS^- and S^{-2}, which are otherwise stable in the in-situ Castile brines under observed Eh conditions.

(c) pH, bicarbonate and specific conductance shifts noted for WIPP-12 are suggestive of carbon dioxide partial pressure variations subsequent to sample contamination by air or degassing. Reactions such as:

$$CH_4 + 2O_2 \longrightarrow CO_2 + 2H_2O$$

or

$$CO_2(\text{aqueous}) \longrightarrow CO_{2(g)}$$

may be operating to cause variable shifts in the carbonate, bicarbonate and pH balance between field analyzed and laboratory analyzed samples.

3.1.2 Flowed versus downhole samples.

The variabilities in chemical composition between samples collected from vertically isolated brine production zones (downhole) and those samples allowed to coalesce with other formation fluids may be significant. The first order evaluation of this conjecture is evaluated by means of the t-test, in which the means are compared between flowed samples and downhole samples.

Chemical composition differences are noted for the average concentration of the following chemical parameters for flowed versus downhole samples:

(a) pH, total dissolved solids, calcium, lithium, magnesium, sodium, chloride and iron for ERDA-6

(b) pH, lithium, magnesium, bicarbonate, bromide and iron for WIPP-12

It would appear from these observations that changes in chemical concentrations occurred from allowing the Castile brines to flow through the uncased Salado formation. If so, one might conclude that the sampling data from the ERDA-6 and WIPP-12 flow tests are not useful for representing the in-situ Castile conditions. However, upon examination of the variabilities between ERDA-6 and WIPP-12, which are discussed in the next section, it is apparent that the differences between ERDA-6 and WIPP-12 are much more substantial than the difference between flowed and downhole samples. Therefore, the differences between downhole and flowed samples may be due to interferences from other geologic material as discussed in Section 3.2

3.1.3 Core Laboratory versus D'Appolonia laboratory

Sample analyses by Core Laboratory and D'Appolonia laboratory analyses samples collected and analyzed by both Core and D'Appolonia showed differences in the following chemical mean values.

(a) potassium, bicarbonate and sulfate for ERDA-6; flow test-3

(b) pH and magnesium for WIPP-12; downhole

Assuming that the samples were collected under identical conditions, these differences are attributable to differences in analytical procedures or laboratory handling and holding times.

3.2 Differences between ERDA-6 and WIPP-12 Brines

In order to graphically depict the differences between the ERDA-6 and WIPP-12 brines, several ternary and binary plots have been prepared. Only those samples which had all of the chemical parameters analyzed were plotted. It becomes apparent when first attempting to depict the major ionic constituents in a three end member (ternary) plot, that the overwhelming abundance of sodium and chloride as the major cationic and anionic constitutents will tend to mask the variability of the other ions present (e.g., calcium, magnesium, potassium, sulfate, bicarbonate, etc.). In order to overcome this difficulty (at least for the cations), sodium was not included on the ternary plot. Instead a ternary plot of calcium-magnesium-potassium is provided in Figure 1.

In examining the ternary plot, it becomes apparent that the ERDA-6 and WIPP-12 brines show two distinct groupings for the major cations considered. In addition to the t-test probability levels associated with the ERDA-6 and WIPP-12 brines for the three major cations, it is instructive to see which ion is varying the most between ERDA-6 and WIPP-12. Figures 2 through 4 provide

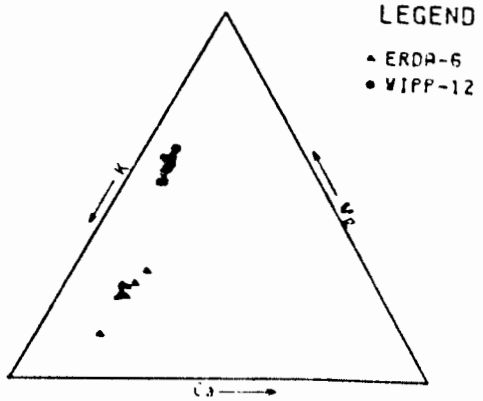

CATION TERNARY DIAGRAM

(EQUIVALENTS)

Figure 1

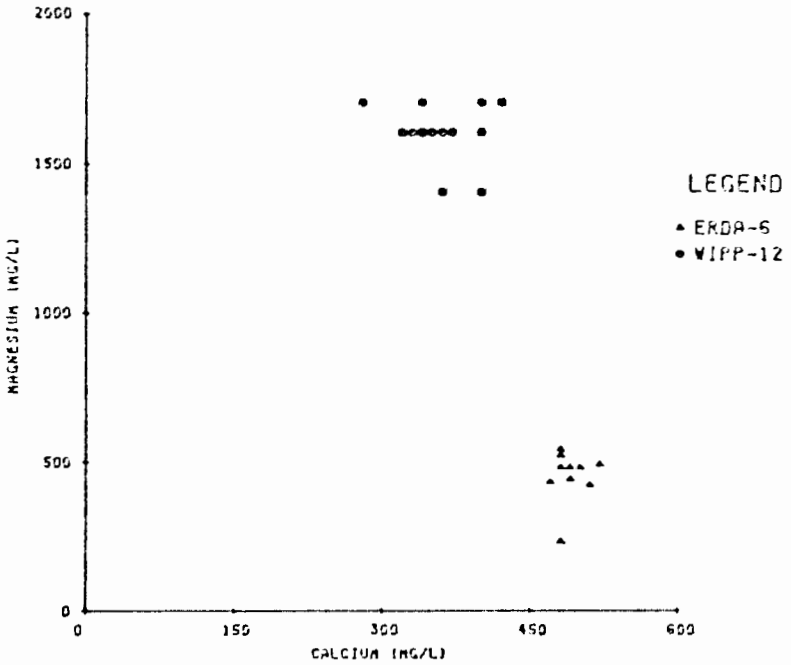

CALCIUM VS. MAGNESIUM

Figure 2

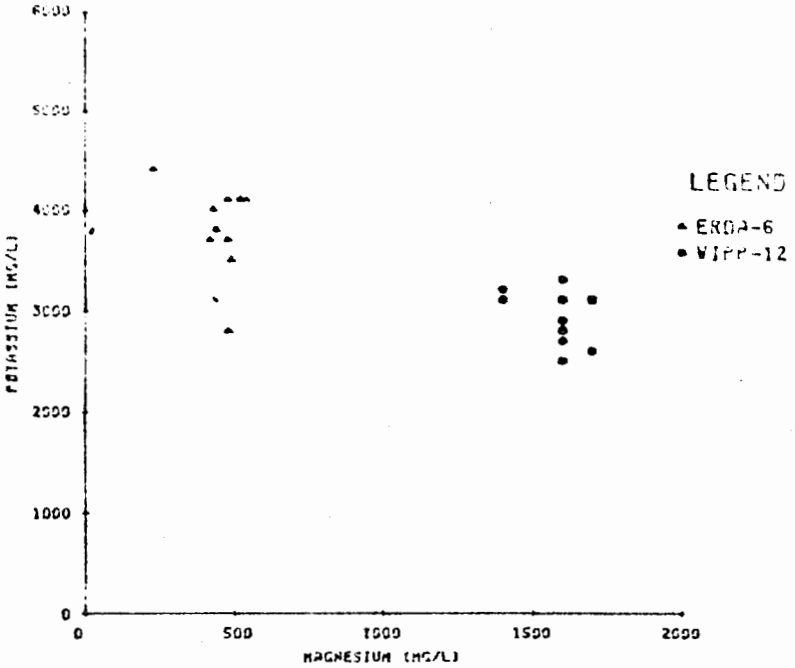

MAGNESIUM VS. POTASSIUM

Figure 3

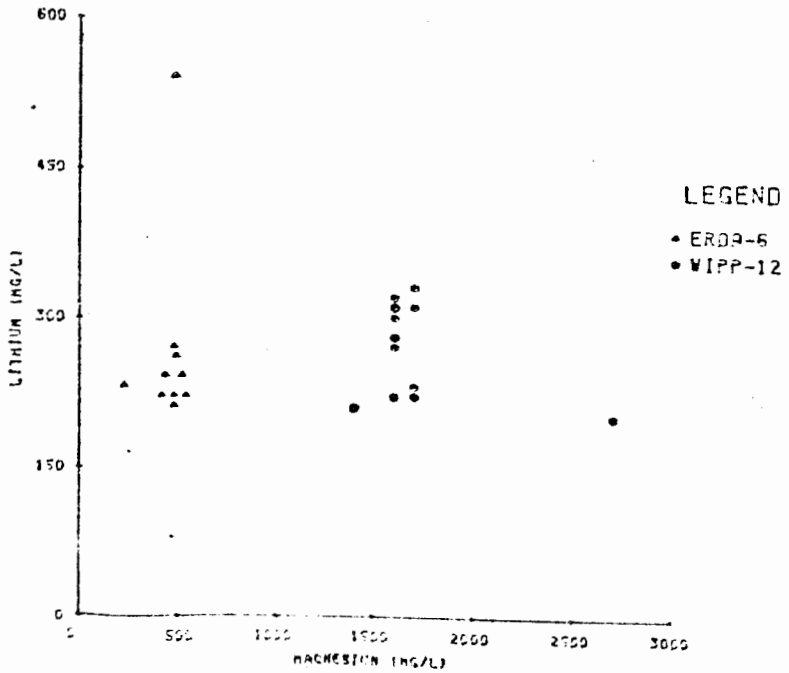

MAGNESIUM VS. LITHIUM

Figure 4

binary plots of calcium vs. magnesium, magnesium vs. potassium and magnesium vs. lithium.

The variability in Cl/Br concentrations are shown on Figure 5. Considerable reliance has been placed on chloride/bromide ratios by many investigators in distinguishing brines that are original trapped seawater (connate water) versus those brines derived by dissolution of halite. Figures 6 through 9 show sulfate vs. calcium, sulfate vs. sodium, chloride vs. sodium and Eh/pH plots for the ERDA-6 and WIPP-12 brines.

As shown in Figures 1 through 4 among the ions considered, magnesium had the greatest variability between ERDA-6 and WIPP-12. This may be due to differences in the degree of dolomitization. As discussed in Section 5, the mechanism of dolomitization is subject to question, although its occurrence is confirmed by petrographic examination.

Figure 6 shows a plot of calcium and sulfate. This plot is a tentative indication that anhydrite solubility is not the only chemical reaction which is controlling the concentration of these two ions in Castile brines. The greater apparent variability in calcium between ERDA-6 and WIPP-12 may be further indication of the variability in the extent of dolomitization between ERDA-6 and WIPP-12.

Finally, Figure 9 indicates a consistent and well defined difference in the Eh/pH environment of ERDA-6 and WIPP-12. WIPP-12 shows a full unit increase in pH and almost 100 mV. more reduced condition than ERDA-6. The fields indicate similar near neutral reducing conditions for both wells, but also show unique or individual groupings. This would be indicative of two different solution buffering environments for ERDA-6 and WIPP-12 brines. The uniqueness of the ERDA-6 and WIPP-12 individual Eh/pH environments would seem to give further evidence to the fact that the ERDA-6 and WIPP-12 reservoirs are not interconnected.

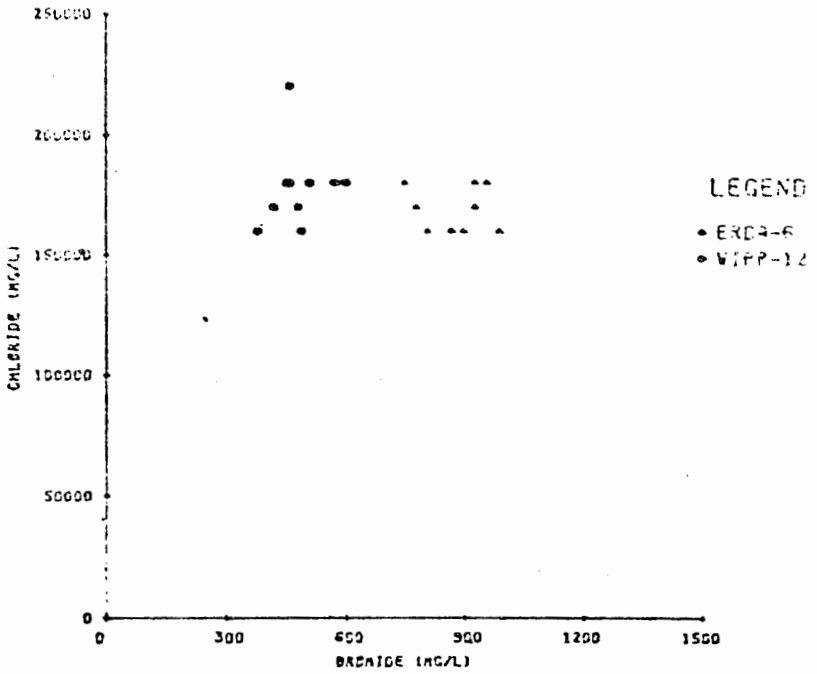

BROMIDE VS. CHLORIDE

Figure 5

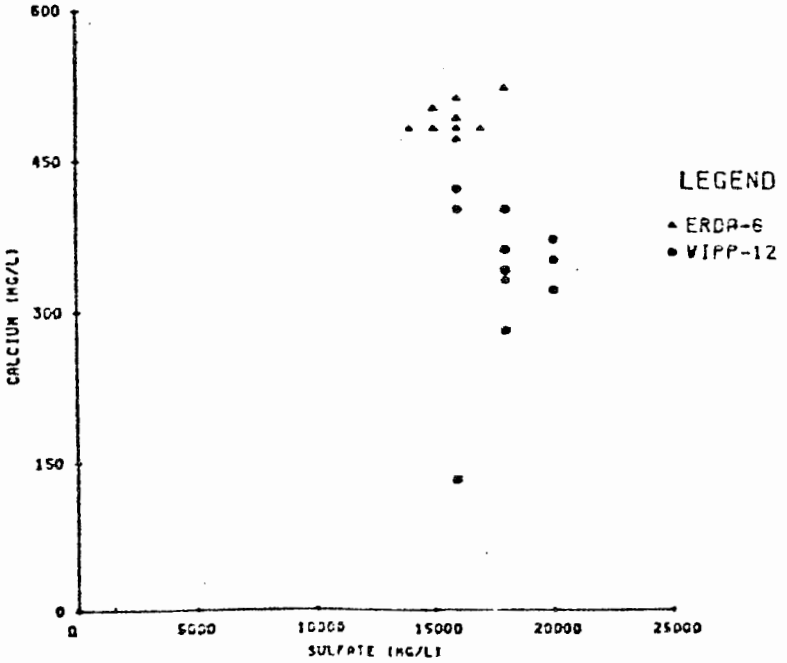

SULFATE VS. CALCIUM

Figure 6

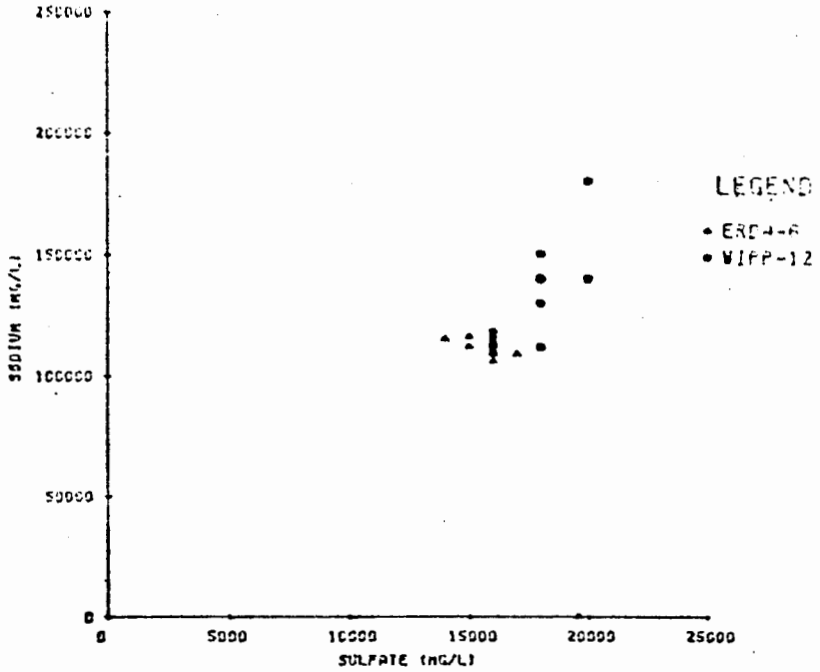

SULFATE VS. SODIUM

Figure 7

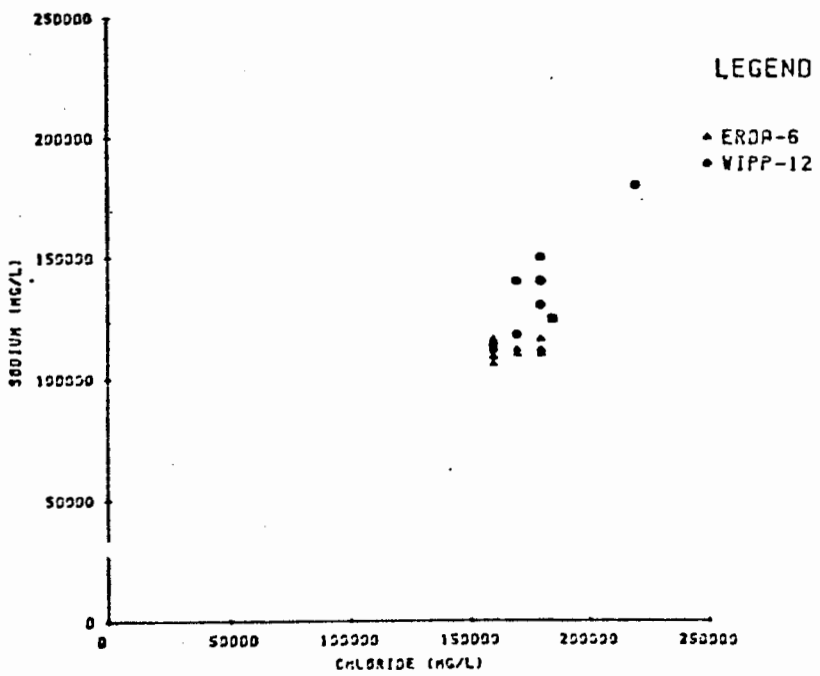

CHLORIDE VS. SODIUM

Figure 8

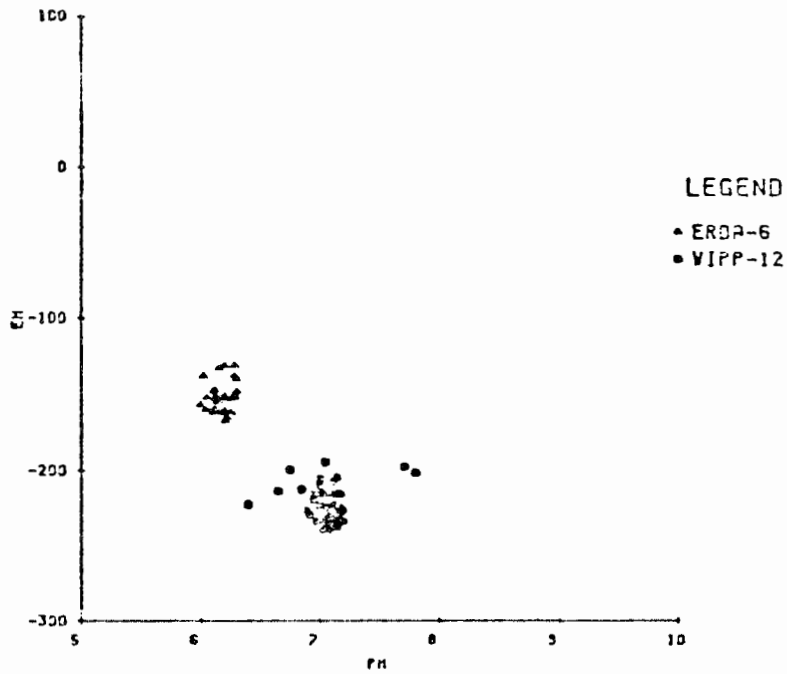

EH - PH FIELD

Figure 9

4.0 BRINE ISOTOPIC FRACTIONATIONS

The data used in this analysis has been published in the "Data File Report ERDA-6 and WIPP-12 Testing" (ref. 1). These data are summarized with explanations in Table 4. For both wells, ERDA-6 and WIPP-12, the average downhole temperature was measured as 26.7°C. This value for the temperature was used in all calculations.

Mechanisms which are believed to be responsible for δD and $\delta^{18}O$ shifts observed in ERDA-6 and WIPP-12 brine have been discussed previously in EEG-18 (ref. 24). It was concluded that the more likely mechanism for the δD and $\delta^{18}O$ shifts is that the brines were derived chiefly from diagenetically modified seawater and/or waters exolved from gypsum dehydration. (See Section 6 for further discussion of seawater modification). The discussion in this section describes the degree to which the isotopic data indicate equilibrium with gas, liquid and solid phases.

4.1 Isotopic thermometers

An isotopic thermometer can be defined as a pair of natural compounds, which contain the same element with more than one isotope, that co-exist (or have been produced) in isotopic equilibrium in the same geochemical system. Faure (ref. 7) points out that the isotopic thermometer is based on three assumptions: (a) the exchange reactions must have reached equilibrium; (b) the isotopic compositions were not altered subsequent to the establishment of equilibrium; (c) the temperature dependence of the fractionation factors is known from experimental determinations. Mathematically, an isotopic thermometer is usually presented by an equation or a plot of the permil fractionation, 1000 ln α versus temperature. The most often encountered expression is as follows:

$$1000 \ln \alpha_{1-2} = A(10^6 T^{-2}) + B \qquad (1)$$

where

α_{1-2} = Isotopic fractionation factor between substance 1 and 2.

T = absolute temperature, °K

A,B = constants obtained from experimental determination.

The isotopic fractionation factor is defined as

$$\alpha_{1-2} = \frac{R_1}{R_2} \qquad (2)$$

there R_1 and R_2 are the ratios of heavy to light isotope in substances 1 and 2. In terms of quantities actually measured in the laboratory (δ-values) this expression becomes

$$\alpha_{1-2} = \frac{1000 + \delta_1}{1000 + \delta_2} \qquad (3)$$

where

$$\delta = \left[\frac{R_{sample}}{R_{standard}} - 1 \right] \times 10^3 \qquad (4)$$

Most permil fractionations can be approximated by

$$10^3 \ln \alpha_{1-2} \simeq \delta_1 - \delta_2 = \Delta_{1-2} \qquad (5)$$

Numerous fractionation factors have been published in the literature and Friedman and O'Neil (ref. 8) have made a compilation of selected permil fractionation for D, ^{18}O, ^{13}C and ^{34}S. The computed fractionations in this report are mostly based on this compilation.

4.2 Isotope Fractionation Factors

Except for the permil fractionations to be discussed below, all calculated permil fractionations are obtained from the compilation of Friedman and O'Neil (ref. 8). For the fractionation of hydrogen between $H_2O(g)$-$CH_4(g)$ we used the two equations for H_2O-H_2 and CH_4-H_2 of Ritchet (ref. 15, p. 263). These equations are respectively:

$$1000 \ln \alpha = -217.3 + 396.8 \times 10^3 T^{-1} + 11.76 \times 10^6 T^{-2}$$

$$1000 \ln \alpha = -238.3 + 289.0 \times 10^3 T^{-1} + 31.86 \times 10^6 T^{-2}$$

The calculated values represent extrapolation since the equations are least square fitting of theoretical data in the temperature range 100-400°C. For the fractionation of oxygen between CO_3^{-2}-(aq)-$CaCO_3$(s) the following equation was used.

$$1000 \ln \alpha = 0.324 \times 10^6 T^{-2} + 0.23$$

This can be obtained from the data in Table 20.1 of reference 7. The calculated value of -861 °/oo for the system $H_2S(g)$ - $H_2O(1)$ is from Table 4 of Friedman and O'Neil (ref. 8). The calculated value is based on a temperature of 25°C. Four values are presented for this system and they can be fitted by the equation

$$1000 \ln \alpha = 53.1 \times 10^6 T^{-2} + 264$$

The value of 1.65 °/oo for the fractionation of sulfur between gypsum and SO_4^{2-} in brine is cited by Faure (ref. 4, p.410) and is attributed to Thode and Monster (ref. 26). Presumably it is also valid for the anhydrite-brine system. For the fractionation of oxygen between dolomite and water the equation of Matthews and Katz (ref. 16) was used:

$$1000 \ln \alpha = 3.06 \times 10^6 T^{-2} - 3.24$$

4.3 Discussion

Table 5 compares calculated permil fractionations for a temperature of 26.7 °C and values observed in the brines of ERDA-6 and WIPP-12.

4.3.1 Oxygen Fractionation

The fractionation of oxygen between the calcite and water does not appear to be in equilibrium for both wells. If the effects of salts in solution are neglected, then the bottomhole temperature of the two wells, ERDA-6 and

WIPP-12, would have to be 50 and 59°C respectively for the observed 1000 ln α(calcite-water) values to indicate isotopic equilibrium. The effects of salts in solution on the fractionation of oxygen cannot be evaluated at this time due to lack of experimental data. Only one paper dealing with the subject could be found in the literature (ref. 27). Since the calculated values for 1000 ln $\alpha(CO_2(g)$-calcite) are greater than the observed values, it cannot be argued that the water in the brines became enriched in $\delta^{18}O$ by interaction with carbonate rock of the Castile Formation. The other three permil fractionations for oxygen indicate equilibrium. The measured value for ERDA-6 of 1000 ln $\alpha(CO_2(g)$ -calcite) appears high. However, the calculated value is an extrapolation obtained from an equation that is fitted to data in the temperature range of 350 to 610 °C.

4.3.2 Carbon Fractionation

The fractionations of carbon for ERDA-6 appear to be in equilibrium. Very good agreement can be obtained for 1000 ln $\alpha(CH_4\text{-}CO_2)$ if one uses α = 0.943, an older value attributed by Faure to Craig (ref. 7, p. 396). The measured values of 1000 ln α(Dolomite-calcite) and 1000 ln $\alpha(CO_3^{2-}$(dissolved)-calcite) for WIPP-12 do not indicate equilibrium. In fact, the dolomite of the core of WIPP-12 is depleted in $\delta^{13}C$ relative to calcite which is contrary to most of the data on natural samples. A depletion of $\delta^{13}C$ in dolomite relative to calcite has been reported by Clayton et al., (ref. 5) for recent carbonate sediments in a lagoon of South Australia and by Tan and Hudson for Jurassic rock of Scotland (ref. 25). The explanation advanced by Clayton et al., for this isotopic behavior is that the two minerals were precipitated under different conditions, and that the dolomite is not formed from calcite by solid-state ion exchange. Tan and Hudson suggest that the dolomite was formed by incorporation of carbon from decaying organic matter. If the dolomite from the core of WIPP-12 formed from the brine, then the explanation of Tan and Hudson suggest that the CO_3^{-2} once had a value of -3.3 °/°° ($\delta^{13}C$).

4.3.3 Hydrogen (deuterium) Fractionation

The calculated permil fractionation of hydrogen between water and methane is lower than the measured value. However, the calculated value is an

extrapolation based on data in the temperature range of 100 to 400°C. Truesdell and Hulston (ref. 9) have provided a graph which indicates computed H_2O-CH_4 deuterium fractionation greater than 200 $^0/_{00}$ at 27^{0}C., which are in better agreement with the observed ERDA-6 and WIPP-12 observed fractionations. The permil fractionations of hydrogen between $H_2S(g)$ and water indicate isotopic equilibrium.

The difference between the calculated and observed values of 1000 ln α (SO_4^{-2}-$H_2S(g)$) has been discussed by Faure (ref. 7, p 404). The observed fractionations of 30 and 24 permil are comparable to data reported in the literature and attributed to biogenic fractionation. However, this explanation has been challenged by Sakai (ref. 22) who, based on calculated isotopic fractionation factors between aqueous sulfide species and sulfide minerals, suggested that the isotopic composition of sulfide minerals may be influenced by the temperature and pH of hydrothermal fluids. Sakai's suggestion was expanded by Ohmoto (ref. 19) who showed that at high temperatures variation in $\delta^{34}S$ values and in $\delta^{13}C$ values of hydrothermal minerals could be caused by slight variation in the oxygen fugacity and/or pH of ore forming fluids during ore deposition. Ohmoto's assumptions have yet to be proven valid for hydrothermal systems at low temperature. For the measured gas compositions at ERDA-6 and WIPP-12, the oxygen fugacities are 10^{-67} atm. and 10^{-69} atm., respectively (ref. 20). If the assumptions of Sakai and Ohmoto are applicable to the Castile brines, then the observed fractionations for sulfur may only indicate the temperatures, fugacities of oxygen, and the pH of the brines rather than the origin of the H_2S.

The fractionation of sulfur between gypsum and sulfate ions in brine indicates equilibrium if it is also valid for anhydrite-brine.

In summary, many of the permil fractionations indicate equilibrium. However, the calcite water fractionation, which does not indicate equilibrium, suggests that the water was not enriched in 18-oxygen by exchange with carbonates of the Castile Formation. The fractionation of carbon between dolomite and calcite for WIPP-12 suggests that the dolomite and calcite are not cogenetic in the sense of having been precipitated from the same solution under the same conditions.

TABLE 4

Isotopic Composition of Brines, Selected Minerals and Gases(1)

Parameters(2)		ERDA-6 Average(3)	ERDA-6 CV(4)	WIPP-12 Average(3)	WIPP-12 CV(4)
Brines					
H_2O					
	δD	-5	50	-0.8	170
	$\delta^{18}O$	9.51	1	10.45	5
SO_4^{2-}					
	$\delta^{34}S$	8.97	5	8.21	2
CO_3^{2-}					
	$\delta^{13}C$	3.96	24	-9.14	38
	$\delta^{18}O$	--	--	10.65	2
Selected Minerals					
Anhydrite, SO_4^{2-}					
	$\delta^{34}S$	11.52	1	11.63	3
Calcite, CO_3^{2-}					
	$\delta^{13}C$	6.41	5	6.70	3
	$\delta^{18}O$	33.76	2	32.38	3
Dolomite, CO_3^{2-}					
	$\delta^{13}C$	--	--	1.67	310
	$\delta^{18}O$	--	--	36.88	2
Gases					
H_2S					
	δD	-570	9	-544	2
	$\delta^{34}S$	- 20.46	3	- 14.36	2
CH_4					
	δD	-264	19	-233	1
	$\delta^{13}C$	- 61.96	4	- 48.65	0.2
CO_2					
	$\delta^{13}C$	- 4.67	41	--	--
	$\delta^{18}O$	51.60	2	--	--

NOTES:

(1) Analyses performed by Global Geochemistry Corporation, Canoga Park, CA.
(2) D, Standard = SMOW.
^{18}O, Standard = SMOW.
^{34}S, Standard = Canon Diablo Triolite (CDT).
^{13}C, Standard = Belemnite From Peedee Formation in South Carolina (PDB).
(3) Average = arithmetic mean.
(4) CV = coefficient of variance (%) = $\frac{\text{Standard deviation}}{\text{average}} \times 100$

TABLE 5

Comparison of Calculated and Measured
Permil Fractionations for ERDA-6 and WIPP-12

Fractionation	Calculated $10^3 \ln\alpha$	Measured--$10^3 \ln\alpha$ ERDA-6	WIPP-12
Oxygen			
$CO_2(g)$ - $H_2O(1)$	40	40.8	--
$CO_2(g)$ - calcite	12	17.1	--
Dolomite - calcite	4.6	--	4.3
Carbonate - water	28.6	23.7	21.4
Dolomite - water	30.8	--	25.8
Carbon			
$CO_3^{=}$(dissolved) - $CO_2(g)$	7.4	8.6	--
$CO_2(g)$ - $CH_4(g)$	68	59.3	--
$CO_2(g)$ - calcite	-11.1	-11.1	--
Dolomite - calcite	2.2	--	-5.0
$CO_3^{=}$(dissolved) - calcite	-3.4	-2.4	-15.9
Hydrogen			
H_2O - methane	-156	-302	-252
$H_2S(g)$ - $H_2O(1)$	-861	-839	-784
Sulfur			
SO_4^{2-} - $H_2S(g)$	68	29.6	22.6
gypsum - SO_4^{2-}	1.65	3.4	2.5

NOTE: all units are permil ($^0/_{00}$)

5.0 URANIUM DISEQUILIBRIUM

The uranium disequilibrium dating method is another tool that is utilized to interpret the evolution of the brine. The data (Table 6) consist of the activity ratio of ^{234}U to ^{238}U for the brine from ERDA-6 and the total uranium concentration for each sample. The governing equations are presented below along with the general solutions. Age estimates are then presented for two separate sets of initial conditions.

Table 6
Uranium Concentration and Activity Ratio
for ERDA-6

	Total Uranium Concentration, ppb	$^{234}U/^{238}U$ Activity Ratio
Brine	.129[1]	1.48 + 0.15[1]
	.224[1]	1.41 + 0.15[1]
	.220[1]	1.50 + 0.15[1]
	2.14[2]	1.37 + 0.07[2]
	1.88[2]	1.33 + 0.07[2]

[1]Data obtained from DOE (Letter of Feb. 14, 1983 from J.M. McGough to R. H. Neill.)

[2]From Powers, et al., (ref. 31, Table 7.27)

5.1 Theoretical Considerations

The equations governing the uranium disequilibrium ratio are as follows:

$$\frac{1}{\lambda_{234}} \frac{d\alpha_b}{dt} = (1 + rf) - \alpha_b \qquad (1)$$

$$\frac{1}{\lambda_{234}} \frac{d\alpha_r}{dt} = (1 - f) - \alpha_r \qquad (2)$$

where

α = activity ratio of ^{234}U to ^{238}U

λ_{234} = decay constant of ^{234}U

f = leach fraction

r = distribution coefficient of uranium between brine and rock

b = a subscript standing for brine

r = a subscript standing for rock

It is assumed that the activity of ^{238}U is constant. For the initial boundary conditions of $\alpha_b = \alpha_{bo}$ and $\alpha_r = \alpha_{ro}$ at t = 0, one obtains the following solutions:

$$(1 + rf) - \alpha_b = [(1+rf) - \alpha_{bo}]\, e^{-\lambda t} \qquad (3)$$

$$(1 - f) - \alpha_r = [(1-f) - \alpha_{ro}]\, e^{-\lambda t} \qquad (4)$$

Combining equations (3) and (4) one obtains the mutually consistent equation

$$f = \frac{\alpha_r(\alpha_{bo}-1) - \alpha_b\,(\alpha_{ro}-1) + \alpha_{ro} - \alpha_{bo}}{[r(\alpha_r - \alpha_{ro}) + \alpha_b - \alpha_{bo}]} \qquad (5)$$

and rewriting equations (3) and (4) one obtains:

$$t = 1.44\, T_{1/2}\, \ell n\, [\frac{\alpha_{bo} - 1 - rf}{\alpha_b - 1 - rf}] = 1.44\, T_{1/2}\, \ell n\, [\frac{\alpha_{ro} - 1 + f}{\alpha_r - 1 + f}] \qquad (6)$$

where $T_{1/2}$ is the half-life of ^{234}U.
When f = 0, equation (6) reduces to:

$$t = 1.44\, T_{1/2}\, \ell n\, [\frac{\alpha_{bo} - 1}{\alpha_b - 1}] = 1.44\, T_{1/2}\, \ell n\, [\frac{\alpha_{ro} - 1}{\alpha_r - 1}] \qquad (7)$$

which is the age equation under conditions of no interaction between rock and brine.

Equations (6) and (7) are general solutions to equations (3) and (4). Two sets of initial conditions are examined. In the first set, the uranium in the rock

is initially at secular equilibrium and the brine initially has an unknown activity ratio, α_0. The second set of initial conditions assumes the rock and the brine had the same initial activity ratio, α_0. The physical interpretation of these 2 sets of initial conditions will be discussed in the following sections.

5.2 Initial Conditions -- Set 1

Initially, the uranium in the rock is assumed to be at secular equilibrium ($\alpha_{ro} = 1$) and the brine is assumed to have contacted the rock with an activity ratio, $\alpha_{bo} = \alpha_0$. Through a combination of uranium deposition from the brine onto the rock and radioactive decay of ^{234}U, the activity ratio of the brine decreases.

When $\alpha_{r1} = 1$ and $\alpha_{bo} = \alpha_0$, equations (5) and (6) reduce to

$$t = 1.44\ T_{1/2} \ln\left[\frac{\alpha_0 - 1 - fr}{\alpha_b - 1 - fr}\right]$$

$$f = \frac{(\alpha_0 - 1)(\alpha_r - 1)}{\alpha_b - \alpha_0 + r(\alpha_r - 1)} \qquad (8)$$

The application of (8) requires the measurement or estimation of α_b, α_0, α_r and r.

The brine activity ratio (α_b) and the rock activity ratio (α_r) have been measured. The data in Table 6 yield an average α_b of 1.46 or 1.35 for ERDA-6 if the most recent uncertified data or the previous (1978) samples, respectively, are used. The more recent α_b for ERDA-6 of 1.46 will be used in subsequent analyses.

The rock activity ratio (α_r) data for ERDA-6 are presented in Figure 10; an α_r of 1.04 appears to be reasonable. It is interesting to note that although α_r varies little, the total uranium in the rock varies over two orders of magnitude depending on where the sample is taken. No α_r data are available for WIPP-12 at this time.

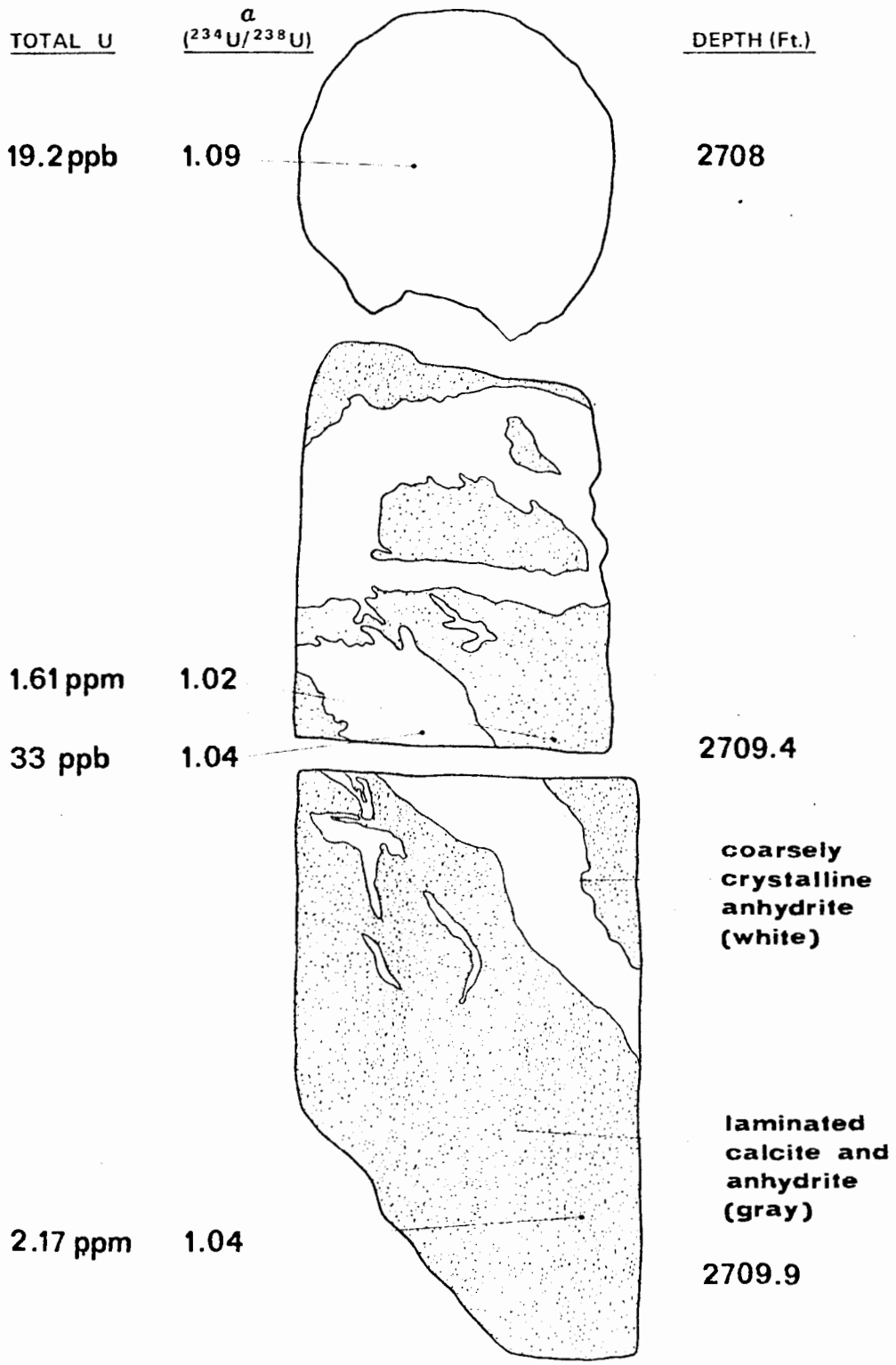

Figure 10

The total uranium concentration and the activity ratio for the rock (αr) in ERDA-6. (From Powers, et al., 1978, Plate 7.52).

The distribution coefficient (r) can be calculated from the measured uranium concentrations in the rock and brine. Table (7) contains estimates of r for various uranium concentrations in the brine and the rock.

Table 7

Estimates of the Distribution Coefficient

for Various Brine and Rock Uranium Concentrations

Brine Uranium Concentration	Rock Uranium Concentration			
ERDA-6	2.17 ppm	1.61 ppm	33 ppb	19.2 ppb
0.129 ppb	16,822	12,481	256	149
0.222 ppb	9,775	7,252	149	86

The initial activity ratio, α_0, is the most difficult parameter to estimate with confidence. Faure (ref. 7) states that for seawater, $\alpha_0 = 1.15$. An α of 5.14 has been measured in the Carlsbad No. 7 well in the Capitan Limestone aquifer; this α has been suggested as α_0 (Powers et al., ref. 31). Powers et al., (ref. 31) citing (Kronfeld et al., ref. 32) indicate that the usual range of α_0 is 10 to 15.

It is obvious that a considerable range of values exist for r and α_0. Consequently, the range of calculated f is quite large. According to Powers et al., (ref. 31, p. 7-96), f = 1 corresponds to 100% leaching, f = -1 corresponds to the case where all the uranium in the rock precipitated from the brine, and f=0 corresponds to the no-interaction case. Table 8 contains f for ERDA-6 for a range of α_0 and r.

Table 8

Estimates of f at ERDA-6

for a Range of α_0 and r

r	α_0 1.15	5.14	10.0	14.2
10	0.0091	-0.061	-0.053	-0.051
50	0.0027	-0.139	-0.069	-0.049
86	0.0016	0.486	-0.097	-0.072
149	0.00097	0.058	-0.293	-0.111
256	0.00057	0.023	0.118	-1.08
3000	0.00005	0.0014	0.0032	0.0048
7252		0.0006	0.0013	0.0019
16,822			0.00054	0.0008

The absolute value of f x 100 gives a measure in percent of the magnitude of rock-brine interaction. For ERDA-6 the negative f (indicating uranium movement from the brine to the rock) range is from 5 to 30 percent. At positive f, the range is from almost zero (at large r) to almost 50%. Note that r<50 for ERDA-6 is less than the lowest possible value from the observed data (Table 8). These data are included for comparison because r = 16.4 was used in the Power et al. (ref. 31) for ERDA-6.

The range of f in Table 8 covers a wide range of possibilities. Absolute values of from 0 to 50 percent correspond to no interaction at 0 to a significant brine-rock interaction at 50 percent. The positive and negative values imply that uranium leached from or deposited into the rock from the brine. Simply, the range of α_0 and r, when combined to yield f, cover a range of values that include almost all possibilities. Additional information is needed in order to evaluate the data. The calculated ages will help narrow the range of possibilities.

5.2.1 Age Calculations

The age of the brine is calculated using equation (8). The use of the word age must be qualified in order to arrive at a correct interpretation of the results. Age in the context of this method refers to the time since "something" has occurred to reset the uranium clock. The fact that the uranium activity ratio is other than a value of one indicates that the brines have not been immobilized and completely isolated at their present location since Permian time. The cause of the uranium disequilibrium is embodied into the initial conditions assumed. These causes will be discussed in Sections 5.2.2 and 5.3.2. The brine ages, in years, are presented in table 9 for the range of α_0 and r given above.

Table 9
Age of ERDA-6 Brine

r	α_0 1.15	5.14	10.0	14.2
		Years		
10	*	5.3×10^5	8.1×10^5	9.4×10^5
50	*	1.4×10^5	4.1×10^5	6.0×10^5
86	*	*	2.4×10^5	3.8×10^5
149	*	*	6.3×10^4	2.0×10^5
256	*	*	*	1.6×10^4
1000<r	*	*	*	*

*indicates a negative age

The data in Table 9 help narrow the range of possibilities presented in Table 8. Only negative values of f produced positive ages. This indicates that if interactions are taking place, uranium from the brine is depositing in the rock. For any particular α_0, the more interaction (indicated by larger absolute f) the younger the age. By ignoring interactions (f=0) a maximum age is obtained. Note that an α_0 of seawater of 1.15 produces no positive age in

Table 9; a similar result occurs if no interaction is assumed.

5.2.2 Discussion--Initial Condition--Set 1

The calculated age is always a maximum, for a particular α_0, when no interactions are assumed (f=0). When interactions are included, positive ages are obtained only for the case where uranium precipitates from the brine onto the rock. In addition, increasing rock brine interaction, as indicated by increasing absolute values of negative f in Table 8, yields decreasing ages. It is clear that as ^{234}U is removed from the brine by precipitation, the ^{234}U content of the brine decreases faster than if radioactive decay alone removed ^{234}U from the brine.

The assumed initial conditions imply that brine with a high disequilibrium has come in contact with rock at secular equilibrium within the last million years or so. The source of the brine is not specified; only the initial uranium activity at the time the brine contacted the present host rock. The only conclusion that can be drawn from these calculations is that the brine has not been isolated within the present fracture system for more than one million years. Whether the brine has moved 5 feet or 5 miles is unresolved based on the above calculations alone.

5.3 Initial Conditions -- Set 2

The initial activity of the rock and the brine are assumed equal in this second set of initial conditions. These conditions imply that at t=0, the rock precipitated from the brine and that subsequent differences in the activity ratios of the rock and brine are due to either precipitation or leaching.

If $\alpha_{ro} = \alpha_{bo} = \alpha_0$, then equation (5) reduces to

$$f = \frac{(\alpha_r - \alpha_b)(\alpha_0 - 1)}{r\,(\alpha_r - \alpha_0) + \alpha_b - \alpha_0} \qquad (9)$$

In all practical cases, $r(\alpha_r - a_0) >> \alpha_b - \alpha_0$ and equation (9) can be rewritten as:

$$rf = \frac{(\alpha_r - \alpha_b)(\alpha_0 - 1)}{(\alpha_r - \alpha_0)} \qquad (10)$$

Equation (10) is significant for it indicates that the calculation of the age of the brines, equation 6, only requires the following three parameters; α_r, α_b, and α_0.

Finally, if there is equilibrium between the brine and the rock and $\alpha_b = \alpha_0$, then equation 1 reduces to

$$f = \frac{1}{r}(\alpha_0 - 1) \qquad (11)$$

5.3.1 Age Calculations

Figure 10, which is taken from Powers et al. (ref. 31), shows fragments from the core of ERDA-6 that was obtained in 1975. The coarsely crystalline white anhydrite (U=33 parts in 10^9 α = 1.04) is considered to be the most recently formed phase. Hence an α_r value of 1.04 will be used in the calculations. The brine samples obtained in 1981 had an α_b value of 1.46 (Table 6). Table 10 summarizes the age of the ERDA-6 brine as a function of α_0 using the precipitation model and the no-interaction model. Therefore, the following equations are used

$$fr = \frac{(\alpha_r - \alpha_b)(\alpha_0 - 1)}{(\alpha_r - \alpha_0)}$$

$$t(\text{interaction}) = 1.44\, T_{1/2} \ln \left[\frac{\alpha_0 - 1 - rf}{\alpha_b - 1 - rf}\right]$$

$$t(\text{no interaction}) = 1.44\ T_{1/2}\ \ell n\ \left[\frac{\alpha_0 - 1}{\alpha_b - 1}\right]$$

As can be seen the interaction model indicates ages greater than one million years even for low values of α_0.

Table 10

Age of the ERDA-6 Brine (years)

α_0	fr	Age Based on Interaction Model	Age Based on No Interaction Mode
1.15	0.5727	4.6×10^5	*
1.5	0.4565	9.1×10^5	3.0×10^4
2.	0.4375	1.2×10^6	2.8×10^5
5.	0.4242	1.7×10^6	7.8×10^5
10	0.4219	2.0×10^6	1.1×10^6

*indicates a negative age

In fact, because f << 1, the ages for the interaction model could have been approximated by equation (6).

$$t = 1.44\ T_{1/2}\ \ln\left[\frac{\alpha_0 - 1}{\alpha_r - 1}\right]$$

which indicates that leaching of activity from the rock does not cause a significant change in the rock activity ratio even for the most recently precipitated coarsely crystalline white anhydrite (Figure 10) because the rock total uranium concentration is so much greater than that of the brine.

5.3.2 Discussion -- Initial Conditions -- Set 2

The results obtained from set 2 are the opposite of those from set 1. The no interaction case yields a minimum, not a maximum age and leaching, not deposition, of uranium from the rock is the predicted rock-brine interaction. Also increased leaching, as indicated by larger fr in Table 10 yields larger ages. The influx of ^{234}U from the rock tends to counter the loss of ^{234}U due to radioactive decay, so the brine ^{234}U is greater than expected.

As in the case of set 1, the results indicate that something has upset the expected secular equilibrium within the last 2 million years. The cause of the disequilibrium could be brine migration into fresh fractures, increased fracturing within the area of the brine without brine migration, or simply continued leaching from existing fractures. Again the only positive conclusion is that the brine was not completely immobile or chemically isolated for the last 2 million years. No conclusion on the origin or true age of the brine can be drawn.

5.4 General Discussion of Uranium Disequilibrium

The disequilibrium models presented above are not intended to precisely depict the actual situation, but rather to place limiting bounds on the evolutionary history of the brines. The choice of the initial conditions dictated whether the model would predict leaching or precipitation of uranium for the same observed data. Based only on physical evidence, the conclusion of leaching is much more likely than the conclusion of precipitation.

The evidence in favor of leaching is really negative evidence against precipitation. The laminated calcite and gray anhydrite in the ERDA-6 core is obviously not reprecipitated. The coarsely crystalline anhydrite precipitated in the fractures has a total uranium concentration 10 to 250 times that of the brine. To precipitate that anhydrite from the present brine would presume uranium preferentially comes out of solution during the deposition of anhydrite. In support of the precipitation conclusion, the measured rock activity ratios are greater than one, indicating enrichment of ^{234}U. The apparently old, laminated portion of the core had a measured α_r of 1.04.

This is most probably within the error of measurement. The laminated portion of the core has a uranium concentration approximately 100 times greater than the coarsely crystalline portion. The error of measurement would be expected to increase with decreasing total uranium concentration, so the largest α_r of 1.09 measured for the coarsely crystalline portion of the core is also within the error of measurement. If one makes the assumption that the rock is greater than 2 million years old, then the rock activity can be considered essentially equal to one.

The preferential leaching of ^{234}U from the rock without significant changes in the α_r is easily explained by examining the total uranium concentrations of the rock and brine. The laminated anhydrite has nearly 10,000 times the total uranium of the brine. A small amount of ^{234}U leached from a fracture would significantly effect the brine activity ratio yet have a negligible effect on the rock activity ratio. The age obtained from a leaching conclusion may be an indication of the age of fracturing. Conversely, the ages may be meaningless if leaching is a continuous process.

In conclusion, the only undisputed fact from the uranium disequilibrium data is that the brine uranium is not in secular equilibrium. This fact suggests that the brine has been a stagnant, chemically isolated body of fluid for no more than about 2 million years. The disequilibrium of the brine probably results from the preferential leaching of ^{234}U from rock fractures. Without additional evidence, neither the true age of the brine, nor the age of fracturing is determinable.

6.0 MAJOR AND MINOR ELEMENT CHEMISTRY

Aside from inferences which may be drawn regarding the chemical sampling statistics which were discussed in Section 3.0, interpretation of the major and minor element chemistry with respect to its diagenesis and relation with its host rock environment provide additional evidence of the history and origin of the Castile reservoir brines (see ref. 24).

Two approaches are discussed for examining some of the brine chemistry. The first area covers the degree to which the brine has equilibrated with its host rock environment and the second examines some of the major/minor chemical relations.

6.1 Equilibrium Thermodynamic Modeling

Some of the applications and limitations of chemical fluid/solid equilibrium models are reviewed together with the work performed by D'Appolonia on the ERDA-6 and WIPP-12 brines.

6.1.1 Background and application

Pioneering work in the area of multicomponent fluid and solid phase equilibrium modeling was described by Garrels and Thompson, (ref. 10); Helgeson, (ref. 13); Helgeson, et al., (ref. 14) and Helgeson, et al., (ref. 12). These early equilibrium models utilized experimentally determined thermodynamic properties of various solid phase minerals in low ionic strength fluids and empirically determined fluid and ion species constants to predict the degree to which a given fluid was in equilibrium (i.e., undersaturated or saturated) with a particular solid or group of solid phase minerals. A fundamental difficulty with the utility of these early models was the degree to which observed versus actual chemical activity of dissolved ion species could be predicted. Nearly all of the early models have relied on various forms of the Debye-Huckel equation for predicting activity coefficients for dissolved ion species and complexed ion species in solution. In dilute aqueous solutions,

the Debye-Huckel equations provided reasonably accurate corrections for ion activities.

However, significant departures from predicted activities have long been noted by workers in the field of equilibrium modeling for solutions concentrated in dissolved soluble ion components. Pitzer (ref. 33), however, was able to provide additional empirical corrections to the Debye-Huckel type equations by providing third and fourth order virial coefficients for single and binary component solutions. Harvie and Weare (ref. 11) were able to extend the earlier free energy model of Pitzer's to include the multi component system $Na-K-Mg-Ca-Cl-SO_4-H_2O$ for solution concentrations which bracket the anticipated ionic strengths of evaporating seawater brines. Thus, the Harvie and Weare model is thought to be one of the most suitable computer equilibrium models for predicting the degree to which a host rock and fluid have "equilibrated" chemically for solutions which are typified by the Castile brines (i.e., high ionic strength). Some of the implicit fundamental assumptions involved in using the model are:

(a) temperature and pressure variations from standard conditions (25^oC and 1 atm.) do not affect the predicted results.

(b) the thermodynamic data for the various solid phases and, thus, their respective solubilities which are used in the model are correct.

(c) analytical data is a correct approximation of true in-situ fluid composition.

6.1.2 Limitations of Equilibrium Modeling

In Section 3 it was brought out that there were several chemical parameters for which the degree of variability between the means of different sample populations were significant. Within the context of limitation (c) above, it is often useful to provide equilibrium computations for all or a large number of sample data so that one may examine trends in data either toward or away from saturation with the mineral phases considered. D'Appolonia has provided ranges of results of equilibrium modeling on selected sets of sample data,

which although useful, do not provide a complete picture of the trends of all available data with respect to mineral saturation.

In the case of limitation (a), or the temperature pressure deviations from standard conditions, the degree to which the Harvie and Weare model is an accurate representation of in-situ Castile conditions may be questioned. In-situ temperatures in the Castile reservoir are on the order of 27°C. Small temperature shifts from 25°C are not anticipated to cause extreme departures from standard condition predictions. However, pressure increases above 1 atm. may be considered to play an important role in buffering the solute/solid relations predicted by the Harvie and Weare model.

The gas phase components CO_2, CH_4 and H_2S all participate in gas/fluid (g/a) exchange reactions, which are dictated by their partial pressures and fugacities under in-situ conditions. For reactions such as:

$$CO_{2(g)} + H_2O \rightleftharpoons H_2CO_{3(a)}$$
$$H_2CO_3 \rightleftharpoons H^+ + HCO_3^-$$
$$HCO_3^- \rightleftharpoons H^+ + CO_3^{2}$$

or

$$CH_{4(g)} + 2O_{2(g)} \rightleftharpoons CO_{2(g)} + H_2O$$

and

$$H_2S_{(g)} + H_2S_{(a)} \rightleftharpoons H^2 + HS^-$$
$$H_2S_{(a)} + 4H_2O \rightleftharpoons SO_4^{-2} + 10H^+ + 8e^-$$

Because the gas phase components described above are used in describing solid-liquid-gas phase equilibrium relations, it is important to determine how the gas phase partial pressures were incorporated into the Harvie and Weare model. Additionally, the original work by Harvie and Weare did not include carbonate solid, ion species or gas phase components.

Based on conversation with William Coons, a geochemist with D'Appolonia, the ERDA-6 and WIPP-12 equilibrium modeling incorporated two methodologies to overcome these apparent difficulties. First, the carbon dioxide partial pressures were back-calculated by adjusting the pH within a range which approximated anticipated downhole pH's. (Note: CO_2 degassing during sampling

will raise pH above in-situ conditions.) By fixing the pH, downhole pressure and total carbonate alkalinity, a partial pressure of CO_2 is derived. Additional thermodynamic data available from Harvie (one of the original authors of the Harvie and Weare equilibrium model) was incorporated in the model to allow distribution of carbonate ion species among competing reactions in order to overcome the original model deficiency.

6.1.3 Results of Equilibrium Modeling

A frequently employed technique for describing the degree to which a fluid has equilibrated with its host rock environment is through the use of the saturation index. For a given solid, a solubility reaction is written as (for example):

$$CaSO_4(s) \rightleftharpoons Ca^{+2} + SO_4^{-2}$$

with the solubility product as

$$K_{sp} = \log \frac{[Ca^{+2}][SO_4^{-2}]}{[CaSO_4(s)]}$$

where the brackets denote the chemical activity of the ions or solid (molality in dilute solutions). Solids are, by convention, assumed to have an activity of unity. Each solid mineral phase (e.g., halite, anhydrite, calcite, etc.) has a unique solubility product for a given pressure and temperature. If the ion activity product (i.e., $[Ca^{+2}][SO_4^{-2}]$ in our example) equals or exceeds the solubility product, then the solution is said to be saturated or supersaturated with respect to the solid phase under consideration.

The Harvey and Weare equilibrium model (and other similar equilibrium computer models) utilize a series of simultaneous equations to distribute the ion species among competing solid phase reactions and ion species in solution to determine the ion activity product for various dissolution/precipitation reactions. The ion activity product when divided by the solubility product then results in a value which is less than unity, unity or greater than unity

depending upon whether the solution is undersaturated, saturated or oversaturated with respect to a given solid phase mineral, respectively.

D'Appolonia has provided results of computed ranges of ion activity and solubility products for five solid phase components of the Castile host rock environment. These data are plotted as fields on Figures 11, 12 and 13. These figures indicate that:

(a) ERDA-6 and WIPP-12 are both saturated with calcite, anhydrite, glauberite and dolomite.

(b) ERDA-6 is undersaturated with halite and WIPP-12 is nearly saturated with halite.

Within the limitations of the Harvie and Weare model that were previously discussed, it appears that the Castile brines are at equilibrium or very near equilibrium with the major rock forming minerals (halite and anhydrite) of the Castile and Salado Formations. With the exception of glauberite, the minerals which are predicted to be in equilibrium with the brine have been verified by petrographic observation from cores and thin sections from cores. Thus, the potential for dissolving additional halite or anhydrite is minimal, assuming the validity of the Harvie and Weare model.

6.2 Major/Minor Brine Chemistry Interpretation

A major role of the brine chemistry data is to aid in determining the history of the Castile brine genesis or evolution from seawater or mixtures of seawater and other water sources. Chief among the "other sources" of water to an evaporating seawater brine are meteoric waters and mineral dehydration (gypsum) waters, although dehydrated water also may owe its original source to an evaporating seawater brine.

6.2.1 Bromide Ratios

Rittenhouse, (ref. 21); Valyashko, (ref. 28) and Collins, (ref. 6) have used the solution and solid chemical properties of bromide as a tool for describing

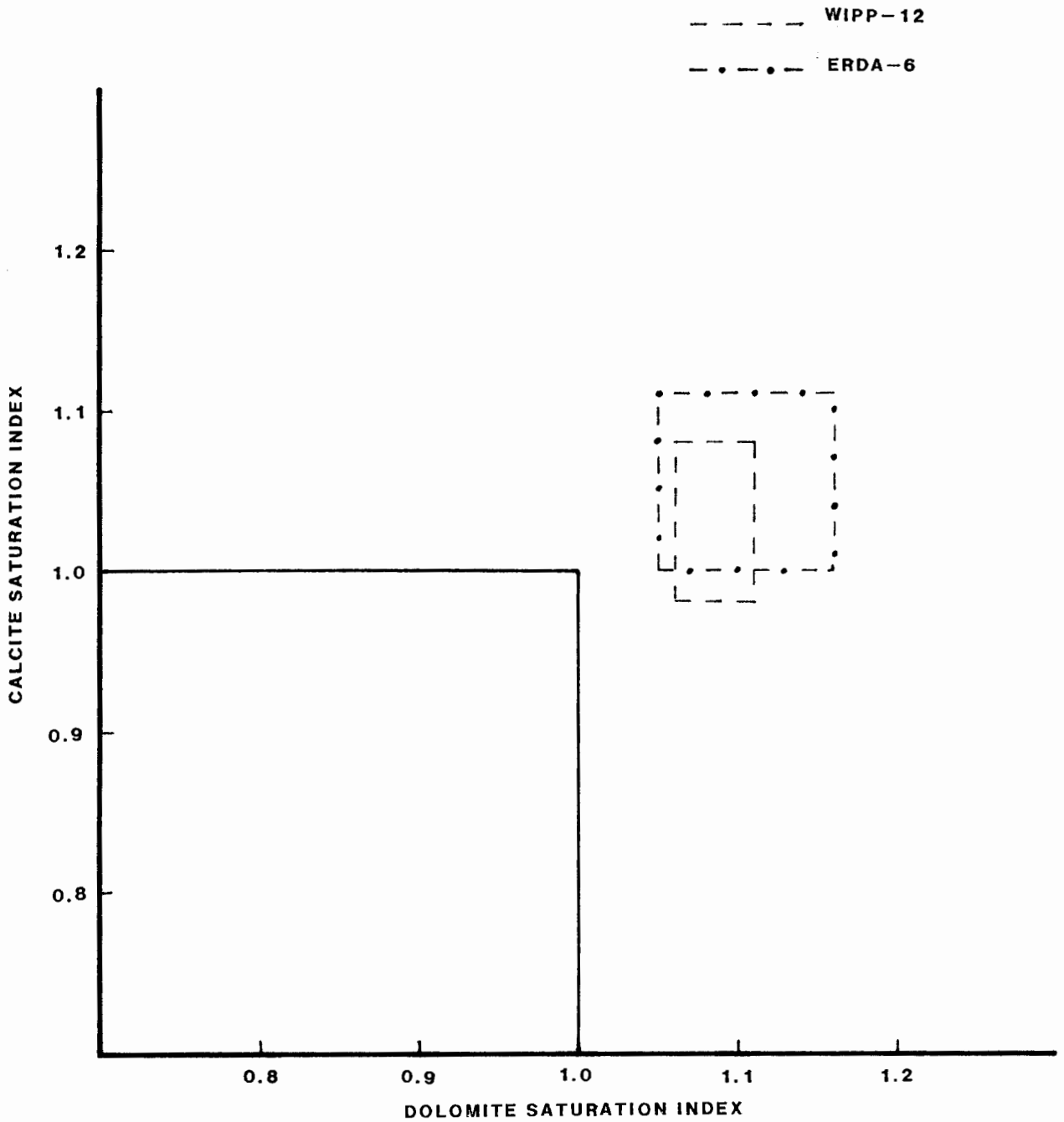

FIGURE 11

CALCITE/DOLOMITE SATURATION INDEX

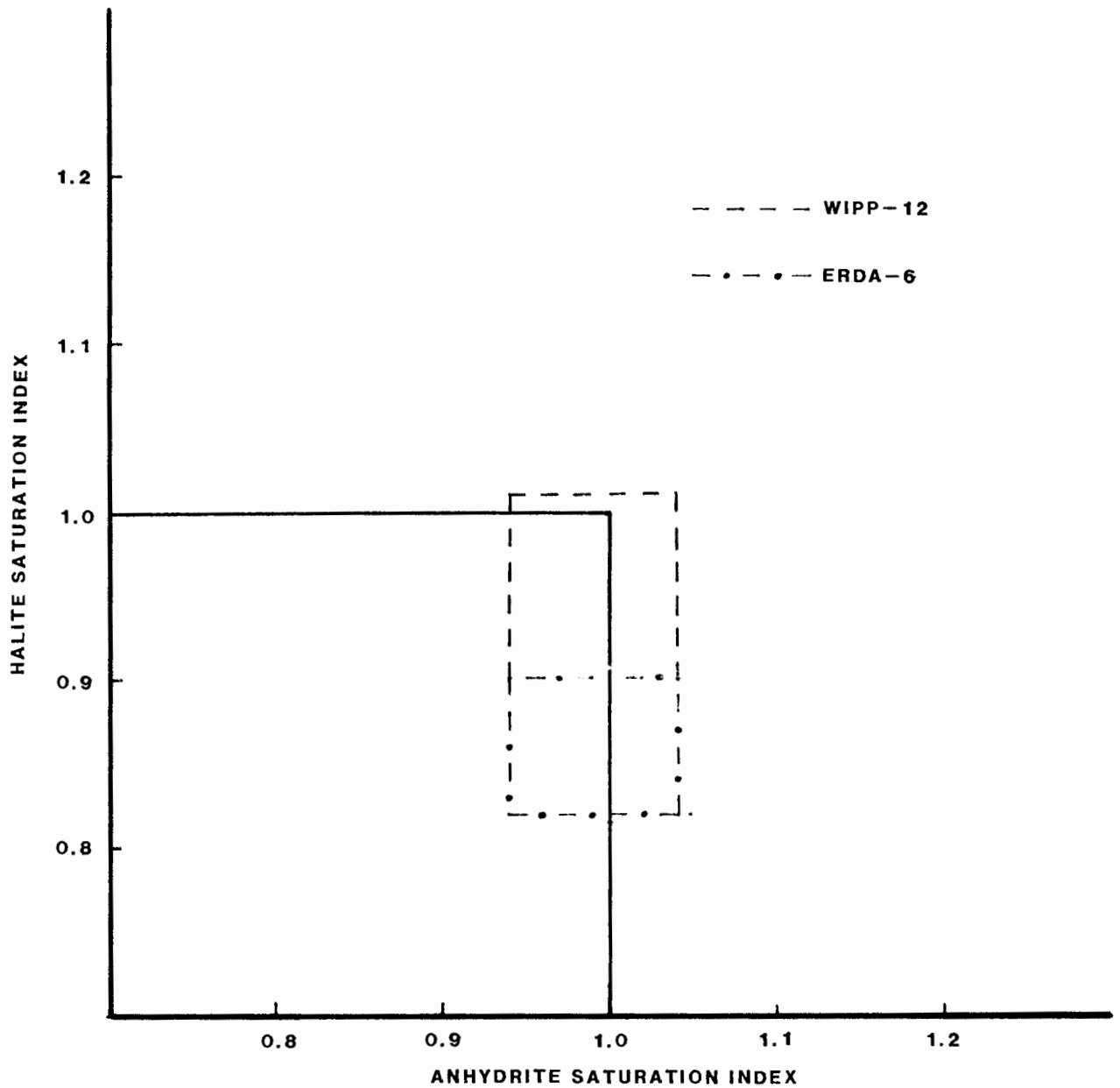

FIGURE 12

HALITE/ANHYDRITE SATURATION INDEX

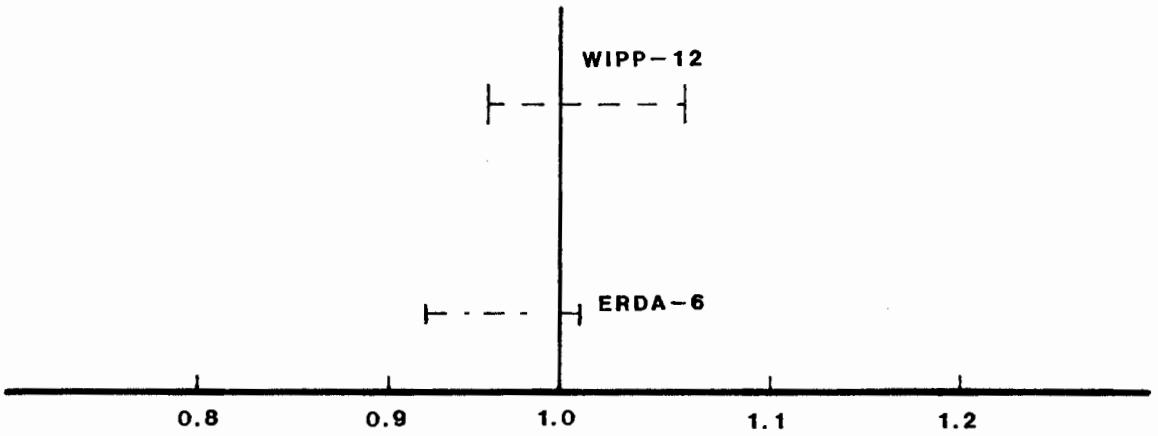

FIGURE 13

GLAUBERITE SATURATION INDEX

the genesis of numerous oilfield and other brine occurrences around the world. The fundamental physio-chemical phenomenon utilized in interpreting bromide chemistry in brines is that bromide is selectively excluded from the crystal lattice of halite which is precipitated during evaporation of seawater and other brines. The result of this phenomenon is that bromide becomes increasingly concentrated in brines during halite precipitation. By comparing the ratio of bromide with other ions in solution, one may draw certain inferences with respect to the evolution of the brines.

Rittenhouse, (ref. 21) has described five groups of brines according to their respective ranges within plots of TDS versus bromide. These five groups of brines are:

(1) those in which the Br and TDS values approximate those brines resulting from a simple concentration of seawater or its dilution with low TDS waters;

(2) those in which the bromide content is elevated above the ratios anticipated for group 1 brines. The increase in bromide is attributed to bromide increases occurring during early compaction and diagenesis and may accompany organic decomposition;

(3) those in which the TDS is higher than the group 1 brines with lowered bromide contents which is attributable to halite dissolution;

(4) those in which the TDS is lower than that expected from evaporating seawater but with bromide contents less than would be expected by simple dilution of evaporating seawater with low TDS waters. Perhaps these are group 3 waters which have been diluted; and

(5) those which are composed of highly saline waters with high TDS and bromide above the concentration of straight seawater evaporation--possibly attributed to bitterns remaining after precipitation of halite and other chloride salts.

Within these five groups of brines described by Rittenhouse (ref. 21), the ERDA-6 and WIPP-12 brines fall within the group 3 to group 1 range suggesting that the brines have followed closely the ion concentration increases attributable to seawater evaporation and additional halite dissolution. This conclusion is also shared by D'Appolonia in their discussion of bromide and chloride plots in relation to seawater evaporation curves.

A fundamental question must then be asked concerning these conclusions. What is the source of water which dissolved additional halite and resulted in the bromide concentrations which are in the Castile reservoir? Two types of dissolution mechanisms might have occurred subsequent to the original seawater evaporation:

(a) the halite was dissolved in some other location and the brine was transported to its present position and mixed with the in-place evaporated seawater, or

(b) a source of water which was undersaturated with halite was introduced to the evaporated seawater with subsequent dissolution of halite and the resultant brine was later transported to its present position.

The first of these mechanisms suggests that at some time in the past a source of undersaturated water dissolved halite and then migrated toward another brine which theoretically was a concentrated seawater at or below halite saturation. Some geologists (ref. 3) have suggested that the Salado is unconformable with the underlying Castile Formation. Such unconformity would suggest the possibility for subaerial exposure of the Upper Castile during Permian time with resultant exposure to meteoric water. Such undersaturated water could conceivably dissolve halite and later mix with more concentrated seawater brines with the resultant observed TDS versus Br ratios.

The second mechanism suggests that a source of undersaturated water was introduced to the reservoir with halite dissolution occurring in place. This mechanism is favored by those (ref. 4) who support the contention that waters undersaturated with respect to halite from the underlying Bell Canyon aquifer have migrated into the upper Castile with concommitant halite dissolution. Although this hypothesis is conceptually plausible and has been demonstrated to

some extent in the laboratory (ref. 4), there remain some difficulties with this hypotheses regarding amounts and rates of salt to be transported and the isotopic contents of deuterium/oxygen-18 in the resulting brine. However, this mechanism may be contributing to some extent to the dissolution of halite. D'Appolonia (ref. 2, pgs. C-33-34) has considered mechanisms of deriving the observed Castile brine chemistry through equilibrium modeling which considers waters of the Bell Canyon aquifer or Salado as the starting solution compositions. Their results indicate that chemical mass balance inconsistencies arise when attempting to verify the evolution of Castile brine chemistry from initial solutions compositions which approximate the brine encountered above (Salado) and below (Bell Canyon) the Castile. Langmuir (ref. 30) has pointed out that both the isotopic differences and the major ion ratio differences between the Castile brines and adjacent (Bell Canyon, Salado and Rustler) formation are of sufficient magnitude to preclude interconnection within the last several million years. These results indicate that Castile brines were not predominantly derived from waters of adjacent lithologic and hydrologic units. A second hypothesis regarding the introduction of waters which are undersaturated with halite involves the dehydration of gypsum.

Although there exists experimental evidence to suggest that primary anhydrite (i.e., the calcium sulphate mineral which precipitates from an evaporating seawater) may precipitate in high temperature (40°-70°C) and salinity environments, there is still an overwhelming body of experimental and thermodynamic data which supports the contention that gypsum is the primary precipitate of calcium sulphate saturation.

The experimentally and thermodynamically determined pressure, temperature and salinity boundaries for gypsum dehydration are shown in Figure 14.

Gypsum is one of the several hydrated forms of calcium sulphate which chemically bonds water to its crystal during precipitation from solution. McDonald (ref. 17) and others have shown that at temperatures, pressures and salinities which approximate burial at several thousand feet, gypsum becomes unstable and dehydrates to form anhydrite and free water. Figure 15 shows the typical cycle for primary gypsum deposition from an evaporating brine. Upon burial, gypsum dehydrates to form anhydrite and then upon later uplift and

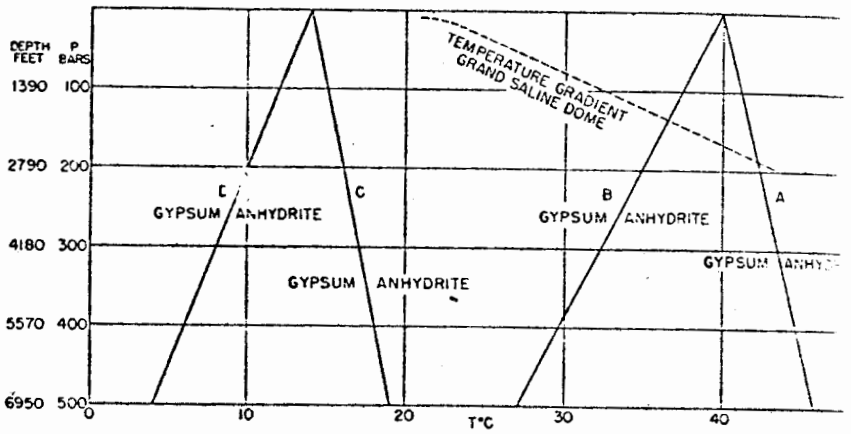

Pressure-temperature relations for the reaction gypsum = anhydrite + water.

Curve A — Same pressure acting on all phases, in presence of pure water

Curve B — Rock pressure acting on solid phases, hydrostatic pressure acting on pure water

Curve C — Same pressure acting on all phases in presence of saturated NaCl solution

Curve D — Rock pressure acting on solid phases, hydrostatic pressure acting on saturated NaCl solution

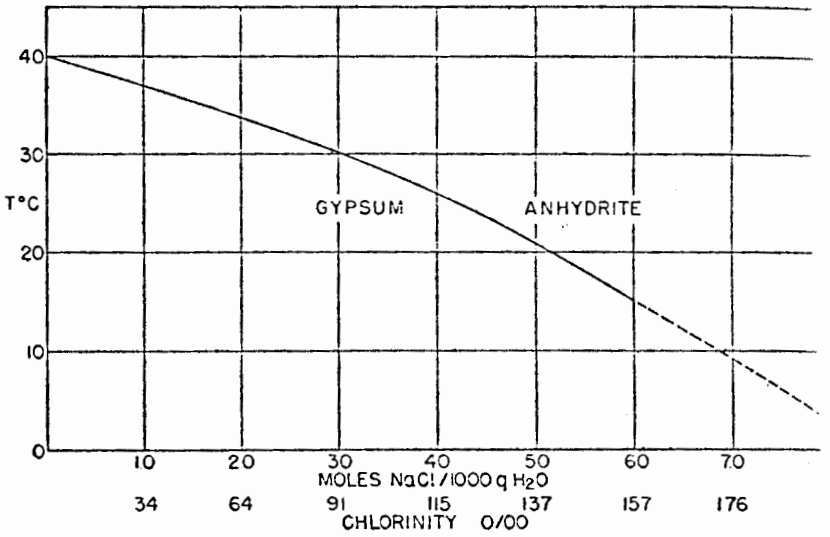

Figure 14

Gypsum - Anhydrite Stability for Various Pressure, Temperature, Salinity Environments (after McDonald, 1953)

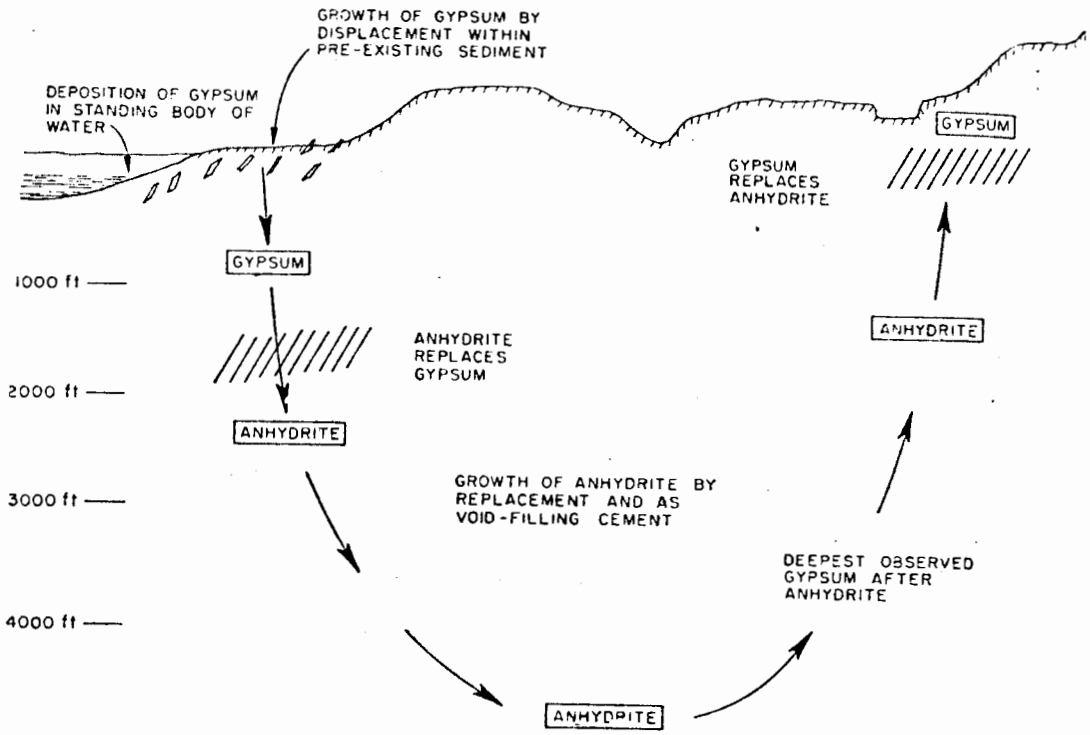

Figure 15

Cycle of Gypsum - Anhydrite Stability
(after Murray, 1964)

exhumation rehydrates to gypsum. After gypsum dehydration at depth, the exolved water is undersaturated with respect to halite and thus may dissolve halite.

This hypothesis is further supported by the δD (deuterium) and $\delta^{18}O$ data for the ERDA-6 and WIPP-12 brines, which fall directly in the fractionation field predicted for waters exolved from gypsum dehydration (ref. 23). Spiegler (ref. 24) indicated that gypsum dehydration may have been a process which produced the $\delta^{18}O$ and δD observed in the ERDA-6 and WIPP-12 brines. This hypothesis was qualified to the extent that subsequent (post dehydration) isotopic modification of $\delta^{18}O$ and δD was minimal. D'Appolonia has stated that this mechanism may be questioned based on the uncertainties regarding the δD and $\delta^{18}O$ content of the Permian seawater and due to the lack of extensive petrographic evidence of anhydrite displaying crystal habits characteristic of gypsum precipitation. The rationale which attributes major differences between Permian seawater δD and $\delta^{18}O$ and its modern SMOW counterpart would cast some doubt as to the validity of gypsum dehydration mechanism as a potential source of brine. However, the information which is available does not provide conclusive proof that there were major oxygen and hydrogen stable isotope shifts in ocean water between Permian and modern seas (ref. 29).

Perhaps a more pertinent question involves consideration of the volume of water which could be derived from dewatering the Castile gypsum prior to its present dehydrated (anhydrite) state, and not one of arguing whether or not gypsum is involved in the Castile brine genesis. The chemical and isotopic data support gypsum as a plausible (if not demonstrable) source of brine occurrence and evolution. It should be noted that if gypsum dehydration were responsible for some portion of the Castile brine evolution, then the reaction has largely been completed (i.e., the Castile has already formed anhydrite) and is unlikely to provide additional water. However, the degree to which gypsum dehydration has provided sufficient volume of water for halite dissolution should be more fully evaluated. Additionally, the pressure and volume changes which accompany gypsum dehydration should be considered as a potential contributing mechanism to reservoir pressurization and possibly fracturing in Anhydrite III.

7.0 CONCLUSIONS

Based on the foregoing discussions and evaluations the following conclusions regarding the upper Castile brine geochemistry are warranted.

(1) The brine chemical data show variability in their mean concentrations among the various sample sets which indicates minor differences in sampling method. These variabilities do not appear sufficient to effect the interpretation of the Castile brine genesis.

(2) The differences in chemical composition between the ERDA-6 and WIPP-12 brines appear to reflect minor differences in the evolution of the brines encountered in the two respective boreholes and not separate origins or sources of original water. The primary differences appear to be in the degree of halite saturation, dolomitization (i.e., replacement of magnesium for calcium in calcite lattices) and mechanisms of gas generation (i.e., biogenic versus thermogenic).

(3) The brines from both ERDA-6 and WIPP-12 appear to be at or near thermodynamic and isotopic equilibrium with the major rock forming minerals of the upper Castile and as such do not appear to have the potential to further degrade the host rock via dissolution. This conclusion is qualified to the extent that the accuracy of D'Appolonia application of the Harvie and Weare thermodynamic equilibrium model is correct subject to further clarification (see Section 4.0 for discussion of limitations).

(4) Major and minor chemistry and chemical ratios (i.e. chloride vs. bromide and TDS vs. bromide) indicate that the Castile brines are derived chiefly from an evaporating seawater source with additional contribution from halite dissolution.

(5) The source of water for the halite dissolution which has already occurred remains unclear. However, because the Castile brines appear to be nearly saturated with halite presently, the need to determine the

original mechanism of halite dissolution may be of academic interest only. Suggested mechanisms for additional halite dissolution include:

(a) dehydration of gypsum at depth;

(b) introduction of meteorically derived water during Permian exposure (Salado/Castile unconformity);

(c) mixing of groundwater from the underlying Bell Canyon aquifer with subsequent isolation by recrystallization or healing of fracture pathways; and

(d) combinations of the above.

8.0 RECOMMENDATIONS

Within the context of long-term repository site integrity, the conclusions stated above are generally supportive of the contention that the Castile brines are stagnant and are not likely to move by dissolution to the WIPP repository. However, because certain of these conclusions are based on interpretive analyses by DOE's technical support contractor (D'Appolonia), some additional clarification from D'Appolonia would strengthen the above conclusions. Thus, it is recommended that the following items be pursued in further detail by DOE and their contractors:

(1) The utilization of the Harvie and Weare equilibrium model to predict the degree to which Castile brines are nearly saturated with ions from the host rock should be clarified by information on:

(a) how the gas phase components of CO_2, CH_4 and H_2S were included to model in-situ Castile conditions of temperature and pressure

(b) how the carbonate solid and soluble phase ions were incorporated into the model.

(2) Although the chemical and isotopic data would seem to indicate that the Castile brines were derived chiefly from an evaporating Permian seawater source, there remains some question as to the mechanism which would allow additional halite dissolution to occur as post-depositional phenomenon. Several mechanisms have been proposed and defended. The degree to which such additional halite dissolution has played in determining the genesis of the Castile brines should be more fully evaluated.

Such evaluation should be made by considering potential mechanisms which would allow water undersaturated with respect to halite to be mixed with water of evaporated seawater brine.

REFERENCES

1. Data File Report - ERDA-6 and WIPP-12 Testing, Waste Isolation Pilot Plant, prepared for Westinghouse Electric Corporation and the U.S. Department of Energy by D'Appolonia consulting Engineers, February, 1982.

2. Brine Reservoirs in the Castile Formation, Southeastern New Mexico, Waste Isolation Pilot Plant, Report No. TME 3153, prepared for Westinghouse Electric Corporation and U.S. Department of Energy, December, 1982.

3. Anderson, R. Y. (1978), Report to Sandia Laboratories on Deep Dissolution of Salt, Northern Delaware Basin, New Mexico.

4. Anderson, R. Y. and D. W. Kirkland (1980), Dissolution of Salt Deposits by Brine Density Flow, Geology, v. 8, p. 66-69.

5. Clayton, R. N., Skinner, H. C. W., Berner, R. A., and Rubinson, M., Isotopic Compositions of Recent South Australian Lagoonal Carbonates, Geochimica Cosmochimica Acta, 32, 983-988, 1968.

6. Collins, A. G., Geochemistry of Oilfield Waters, Elsevier Publishing Company, N. Y., 1975.

7. Faure, G., Principle of Isotope Geology, John Wiley and Sons, New York, 1977.

8. Friedman, I., and O'Neil, J. R., Compiltion of Stable Isotope Fractionation Factors of Geochemical Interest. Data of Geochemistry (Fleischer, M., Ed.) Chapter KK, U.S. Geological Survey Prof. Paper 440-KK, 1977.

9. Truesdell, A.H. and J.R. Hulston, Isotopic Evidence on Environments of Geothermal Systems in, Fritz, P. and J. Ch. Fentes (editors), Handbook of Environmental Isotope Geochemistry Vol. I, Elsevier Publishing Co., N. Y., 1980.

10. Garrels, R. M. and M. E. Thompson (1962), A chemical Model for Sea Water at 25°C and One Atmosphere Total Pressure, Amer. J. Sci., vol. 260, p. 57-66.

11. Harvie, C. E. and J. H. Weare (1980), the Prediction of Mineral Solubilities in Natural Waters: The Na-K-Mg-Ca-Cl-SO_4-H_2O System from Zero to High Concentration at 25°C, Geochimica et Cosmochimica Acta, vol. 44, p. 981-997.

12. Helgeson, H. C. et al., (1970), Calculation of Mass Transfer in Geochemical Processes Involving Aqueous Solutions, Geochimica et Cosmochimica Acta, vol. 34, p. 569-592.

13. Helgeson, H. C., (1968) Evaluation of Irreversible Reactions in Geochemical Processes Involving Minerals and Aqueous Solution - I: Thermodynamic Relations, Geochimica et Cosmochimica Acta, vol. 32, p. 853-877.

14. Helgeson, H. C. et al., (1969) Evaluation of Irreversible Reactions in Geochemical Processes Involving Aqueous Solutions-II: Applications, Geochimica et Cosmochimica Acta, vol. 33, p. 455-481.

15. International Atomic Energy Agency, Stable Isotope Hydrology. Deuterium and Oxygen-18 in the Water Cycle, Technical Report Series No. 210, (Gat, J. R. and Gonfiantini, R., Ed.) IAEA, Vienna, 1981.

16. Matthews, A., and Katz, A., Oxygen Isotope Fractionation during the Dolomitization of Calcium Carbonate, Geochimica et Cosmochimica Acta, 41

17. McDonald, J. F. (1953) Anhydrite-Gypsum Equilibrium Relations, Amer. J. Sci., vol. 251, p. 884-898.

18. Murray, R. C. (1964), Origin and Diagenesis of Gypsum and Anhydrite, J. Sed. Petrol., vol. 34, n. 3, p. 512-523.

19. Ohmoto, H., Systematic of Sulfur and Carbon Isotopes in Hydrothermal Ore Deposits, Econ. Geol., 67, 551-578, 1972.

20. Popielak, R. S., Beauheim, R. L., Black, S. R., Coons, W. E., Ellingson, C. T., and Olsen, R. L., Brine Reservoirs in the Castile Formation, Southeastern New Mexico, U. S. Department of Energy, Albuquerque, (TME 3153), December, 1982.

21. Rittenhouse, G. (1967), Bromine in Oil-Field Waters and its Use in Determining Possibilities of Origin of These Waters, Amer. Assoc. Pet. Geol. Bull., v. 51, no. 12, p. 2430-2440.

22. Sakai, H., Geochimica et Cosmochimica Acta, Isotopic Properties of Sulfur Compounds in Hydrothermal Processes, Geochem. Jour., 2, 29-49, 1968.

23. Sofer, Z. (1978), Isotopic Composition of Hydration Water in Gypsum, Geochimica et Cosmochimica Acta, vol. 42, p. 1141-1149.

24. Spiegler, P., and Updegraff, D., Origin of the Brines from the Drill Holes ERDA-6 and WIPP-12 Based on Stable Isotope Concentrations of Hydrogen and Oxygen, Report EEG-18, March, 1983.

25. Tan, F. C., and Hudson, J. D., Carbon and Oxygen Isotopic Relationship of Dolomites and Co-existing Calcites, Great estuarine Series (Jurassic), Scotland, Geochimica et Cosmochimica Acta, 35, 755-767, 1971.

26. Thode, H. G., and Monster, J., Sulfur-Isotope Geochemistry of Petroleum Evaporites and Ancient Seas. In Fluids in Subsurface Environments, (Yound, A., and Galley, J. E., Eds.) Amer. Assoc. Petrol. Geologists, Mem. 4. pp. 367-377, 1965.

27. Truesdell, A. H., Oxygen isotope activities and concentration in aqueous salt solutions at elevated temperatures - Consequences for isotope geochemistry: Earth and Planetary Sci. Letters, v. 23, no. 3, p. 387-396., 1974.

28. Valyashko, M. G. (1956), Geochemistry of Bromine in the Process of Salt Deposition and the Use of the Bromine Content as a Genetic and Prospecting Criterion, Geochemistry, no. 6, p. 570-589.

29. Kharaka, Y. K. and W. Carothers, Oxygen and Hydrogen Isotope Geochemistry of Deep Basin Brines, in Fritz, P. and J. Ch. Fontes Handbook of Environmental Isotope Geochemistry, Vol. II (to be published).

30. Langmuir, D., Age and Evolutionary History of WIPP-12 and ERDA-6 Groundwaters and their Comparison with Other Groundwaters in the Delaware Basin, Consultant Report to the Environmental Evaluation Group, January, 1983.

31. Powers, D. W., S. J. Lambert, S-E. Shaffer, L. R. Hill, and W. D. Weart, ed. Geological Characterization Report, Waste Isolation Pilot Plant (WIPP) Site, Southeastern New Mexico. SAND 78-1596, Vol. 1, 2 (Albuquerque, NM; Sandia Laboratories), 1978.

32. Kronfeld, K., E. Gradsztajn, H. W. Muller, J. Raddin, A. Yaniv, and R. Zach, Excess ^{234}U: an Effect in Confined Waters, Earth Planetary Sci. Letters, vol. 27, p. 342, 1975.

33. Pizer, K. S., Thermodynamcis of Electrolytes: Theoretical Basis and General Equations. J. Phys. Chem. 77, 268 - 277 (1973).

APPENDIX

SAMPLE POPULATION GROUPS (FOR t-tests)

Number	Description
001	ERDA 6.8; Flow Test 2; laboratory
002	ERDA 6.8; Flow Test 2; field
003	ERDA 6.8; Flow test 2; laboratory/field combined; (1+2)
004	ERDA 6.9; Flow Test 3; laboratory
005	ERDA 6.9; Flow test 3; field
006	ERDA 6.9; Flow test 3; laboratory/field combined; (4+5)
007	ERDA 6.8+6.9; laboratory combined; (1+4)
008	ERDA 6.8+6.9; field combined; (2+5)
009	ERDA 6.8+6.9; laboratory/field combined; (1+2+3+4)
010	ERDA 6.9; downhole laboratory by D'Appolonia
011	ERDA 6.9; downhole laboratory by Core
012	ERDA 6.9; downhole D'Appolonia/Core combined; (10+11)
101	WIPP 12.7; Flow Test 1; laboratory
102	WIPP 12.7; Flow Test 1; field
103	WIPP 12.7; Flow Test 1; laboratory/field combined; (101+102)
104	WIPP 12.19; Flow test 2; field
105	WIPP 12.20; Flow Test 3; field
106	WIPP 12.20; Flow Test 3; field
107	WIPP 12.20; Flow Test 3; laboratory/field combined; (105+106)
108	WIPP 12.7+12.20; Flow Test 1+3; laboratory combined; (101+103)
109	WIPP 12.7+12.19+12.20; Flow Tests 1+2+3; field combined; (102+104+105)
110	WIPP 12.7+12.19+12.20; flow Tests 1, 2, & 3; lab + field combined; (101+102+104+105+106)
111	WIPP 12.7; Downhole; laboratory (Core)
112	WIPP 12.7; Downhole; laboratory (D'Appolonia)
113	WIPP 12.8; Downhole (DST-3020); laboratory (D'Appolonia)
114	WIPP 12.7+12.8; Downhole combined; (111+112+113)

TABLE 1

ERDA-6 and WIPP-12

Sample Statistical Groups

TABLE 2

T-test Results

Brine Parameter	001 - 002			004 - 005			003 - 006			001 - 004		
	t	α	d.f.	t	α	d.f.	t	α	d.f.	t	α	d.f.
pH	5.62	Ø	24	7.20	Ø	19	4.39	.00007	45	1.22	.2b	8
spec. cond.	1.65	.11	24	2.62	.02	18	2.82	.007	44	0.43	.68	8
TDS	-	-	-	-	-	-	1.75	.12	8	1.75	.12	8
Ba^{++}	-	-	-	-	-	-	1.33	.22	8	1.33	.22	8
Ca^{++}	-	-	-	-	-	-	>0	<1.00	8	>0	<1.0	8
Li^{+}	-	-	-	-	-	-	1.67	.13	8	1.67	.13	8
Mg^{++}	-	-	-	-	-	-	0.61	.56	8	0.61	.56	8
K^{+}	-	-	-	-	-	-	1.14	.29	8	1.14	.29	8
Wa^{+}	-	-	-	-	-	-	1.26	.24	8	1.26	.24	8
Sr^{++}	-	-	-	-	-	-	0.16	.88	8	0.16	.88	8
HCO_3	1.50	.15	15	0.02	.98	10	1.31	.20	27	0.55	.60	8
Br^{-}	-	-	-	-	-	-	1.61	.15	8	1.61	.15	8
Cl^{-}	4.70	.0003	15	4.18	.002	10	0.25	.80	27	0.25	.80	8
F^{-}	-	-	-	-	-	-	>0	<1.0	8	>0	<1.0	8
SO_4^{-}	1.33	.20	15	3.97	.003	10	3.34	.002	27	1.76	.12	8
$NH_3(N)$	-	-	-	-	-	-	>0	<1.0	8	>0	<1.0	8
$NO_3(N)$	-	-	-	-	-	-	0.60	.57	8	0.60	.57	8
$PO_4(P)$	-	-	-	-	-	-	>0	<1.0	8	>0	<1.0	8
Al^{++}	-	-	-	-	-	-	0.64	.54	8	0.64	.54	8
B^{+++}	-	-	-	-	-	-	0.17	.87	8	0.17	.87	8
Cu^{++}	-	-	-	-	-	-	0.34	.74	8	0.34	.74	8
Fe^{++}	-	-	-	-	-	-	0.10	.92	8	0.10	.92	8
Mn^{++}	-	-	-	-	-	-	0.45	.66	8	0.45	.66	8
Zn^{++}	-	-	-	-	-	-	0.34	.74	8	0.34	.74	8

TABLE 2

T-Test Results

Brine Parameter	002 - 005			010 - 011			007-012					
	t	α	d.f.	t	α	d.f.	t	α	d.f.	t	α	d.f.
pH	8.52	Ø	35	2.27	.06	6	4.71	.0002	16			
spec. cond.	3.22	0.003	34	-	-	-	-	-	-			
TDS	-	-	-	-	-	-	2.84	.01	12			
Ba	-	-	-	-	-	-	-	-	-			
Ca	-	-	-	2.13	.08	6	9.20	Ø	16			
Li	-	-	-	-	-	-	3.82	.002	12			
Mg	-	-	-	0.87	.42	6	5.60	.00004	16			
K	-	-	-	2.50	.05	6	1.31	.21	16			
Na	-	-	-	29.7	Ø	6	4.56	.0003	16			
Sr	-	-	-	-	-	-	-	-	-			
HCO_3	1.59	0.13	17	3.51	.01	6	14.36	Ø	16			
Br	-	-	-	-	-	-						
Cl	1.81	0.09	17	1.91	0.10	6	2.86	0.011	16			
F	-	-	-	-	-	-						
SO_4	4.86	.0001	17	9.55	Ø	6	0.97	.35	16			
$NH_3(N)$	-	-	-	-	-	-						
$NO_3(N)$	-	-	-	-	-	-						
$PO_4(P)$	-	-	-	-	-	-						
Al	-	-	-	-	-	-						
B	-	-	-	-	-	-	1.09	.30	12			
Cu	-	-	-	-	-	-						
Fe	-	-	-	-	-	-	2.47	.029	12			
Mn	-	-	-	-	-	-						
Zn	-	-	-	-	-	-						

TABLE 2

T-Test Results

Brine Parameter	101 - 102			105 - 106			103-107			101 - 105		
	t	α	d.f.	t	α	d.f.	t	α	d.f.	t	α	d.f.
pH	3.99	.005	7	19.42	>Ø	59	3.86	.0003	68	6.90	00004	10
spec. cond.	0.97	.36	7	12.43	>Ø	59	4.20	>Ø	68	5.28	.0004	10
TDS	-	-	-	-	-	-	1.42	.19	10	1.42	.19	10
Ba	-	-	-	-	-	-	0.92	.38	10	0.92	.92	10
Ca	-	-	-	-	-	-	3.64	.005	10	3.64	.005	10
Li	-	-	-	-	-	-	5.30	.0003	10	5.30	.0003	10
Mg	-	-	-	-	-	-	2.69	.02	10	2.69	.02	10
K	-	-	-	-	-	-	1.11	.29	10	1.11	.29	10
Na	-	-	-	-	-	-	2.54	.03	10	2.54	.03	10
Sr	-	-	-	-	-	-	1.67	.13	10	1.67	.13	10
HCO_3	0.36	.73	7	7.12	>Ø	55	1.68	.10	64	3.41	.007	10
Br	-	-	-	-	-	-	1.74	.11	10	1.74	.11	10
Cl	3.84	.006	7	0.55	.58	55	0.27	.79	61	1.49	.17	10
F	-	-	-	-	-	-	12.91	>Ø	10	12.91	>Ø	10
SO_4	5.49	.0009	7	0.51	.61	55	0.31	.78	61	4.08	.002	10
$NH_3(N)$	-	-	-	-	-	-	3.12	.01	10	3.12	.01	10
$NO_3(N)$	-	-	-	-	-	-	0.05	.96	10	0.05	.96	10
$PO_4(P)$	-	-	-	-	-	-	-	-	-	-	-	-
Al	-	-	-	-	-	-	0.85	.41	10	0.85	.41	10
B	-	-	-	-	-	-	3.60	.005	10	3.60	.005	10
Cu	-	-	-	-	-	-	0.06	.95	10	0.06	.95	10
Fe	-	-	-	-	-	-	2.36	.04	10	2.36	.04	10
Mn	-	-	-	-	-	-	4.85	.0007	10	4.85	.0007	10
Zn	-	-	-	-	-	-	3.34	.007	10	3.34	.007	10

TABLE 2

T-Test Results

Brine Parameter	111 - 112			110 - 114								
	t	α	d.f.	t	α	d.f.	t		d.f.	t	t_c	d.f.
pH	4.99	.04	2	2.72	>0.00	74						
spec. cond.	-	-	-	-	-	-						
TDS	-	-	-	0.15	0.83	13						
Ba	-	-	-	-	-	-						
Ca	2.59	.12	2	0.27	0.79	15						
Li	-	-	-	3.53	.004	13						
Mg	12.83	.006	2	4.98	.0001	15						
K	1.96	.19	2	1.73	.104	15						
Na	2.87	.10	2	1.86	.083	15						
Sr	-	-	-	-	-	-						
HCO_3	-	-	-	6.65	>0.00	70						
Br	-	-	-	2.22	.045	13						
Cl	0.54	.64	2	0.67	.505	70						
F	-	-	-	-	-	-						
SO_4	3.48	.07	2	0	<1.00	65						
$NH_3(N)$	-	-	-	-	-	-						
$NO_3(N)$	-	-	-	-	-	-						
$PO_4(P)$	-	-	-	-	-	-						
Al	-	-	-	-	-	-						
B	-	-	-	0.16	.87	13						
Cu	-	-	-	-	-	-						
Fe	-	-	-	7.23	>0.00	13						
Mn	-	-	-	-	-	-						
Zn	-	-	-	-	-	-						

TABLE 3

Mean, Deviation and Number of Samples

Brine Parameter	ERDA 6.8 (Flow test 2; lab.)			ERDA 6.8 (Flow test 2; field			ERDA 6.8 Flow Test 2 Com		
	$\bar{x}$	s	n	$\bar{x}$	s	n	$\bar{x}$	s	n
pH	6.45	0.15	7	6.23	0.04	19	6.29	0.13	26
spec. cond.	489,000	39,340	7	460,500	36,840	19	454,200	52,510	26
TDS	332,857	7,559	7	-	-	-	332,857	7,559	7
Ba	0.98	0.85	7	-	-	-	0.98	0.85	
Ca	490	16.3	7	-	-	-	490	16.3	
Li	241	19.5	7	-	-	-	241	19.5	
Mg	439	96.9	7	-	-	-	439	96.9	
K	3,943	299	7	-	-	-	3943	299	
Na	110,571	3,155	7	-	-	-	110,571	3155	
Sr	17	2.7	7	-	-	-	17	2.7	
HCO_3	2614	38	7	2535	127	10	2569	109	17
Br	853	73	7	-	-	-	853	73	
Cl	168,571	8,997	7	191,600	9580	10	182094	14893	17
F	1.73	0.11	7	-	-	-	1.73	0.11	
SO_4	16,250	886	7	17,000	1190	10	16,718	1167	17
$NH_3(N)$	870	25	7	-	-	-	870	25	
$NO_3(N)$	603	112	7	-	-	-	603	112	
$PO_4(P)$	0.37	0.08	7	-	-	-	0.37	0.08	
Al	2.19	1.34	7	-	-	-	2.19	1.34	
B	674	117	7	-	-	-	674	117	
Cu	0.47	0.29	7	-	-	-	0.47	0.29	
Fe	3.53	1.57	7	-	-	-	3.53	1.57	
Mn	7.00	0.82	7	-	-	-	7.00	0.82	
Zn	0.56	0.12	7	-	-	-	0.56	0.12	

TABLE 3

Mean, Deviation and Number of Samples

Brine Parameter	ERDA 6.9 (Flow test 3; lab.)			ERDA 6.9 (Field)(Flow test3)			ERDA 6.9 Flow Test 3 Com		
	$\bar{x}$	s	n	$\bar{x}$	s	n	$\bar{x}$	s	n
pH	633	0.04	3	6.10	0.05	18	6.14	0.09	21
spec. cond.	500,000	10,000	3	490,300	4,413	17	488,680	11,600	20
TDS	323,333	5,774	3	-	-	-	323,333	5,774	3
Ba	0.24	0.22	3	-	-	-	0.24	0.22	3
Ca	490	17.3	3	-	-	-	490	17.3	3
Li	220	Ø	3	-	-	-	220	Ø	3
Mg	480	60	3	-	-	-	480	60	3
K	3,533	668	3	-	-	-	3,533	668	3
Na	113,667	3,215	3	-	-	-	113,667	3,215	3
Sr	17.3	1.5	3	-	-	-	17.3	1.5	3
HCO_3	2,633	57	3	2,635	132	9	2,627	120	12
Br	940	62	3	-	-	-	940	62	3
Cl	166.667	11,547	3	185,400	1,854	9	180,808	10,061	12
F	1.73	0.06	3	-	-	-	1.73	0.06	3
SO_4	15,000	1,000	3	21,700	2,604	9	20,383	4,133	12
$NH_3(N)$	870	10	3	-	-	-	870	10	3
$NO_3(N)$	647	28.9	3	-	-	-	647	28.9	3
$PO_4(P)$	0.37	0.05	3	-	-	-	0.37	0.05	3
Al	2.85	1.16	3	-	-	-	2.83	1.16	3
B	660	72	3	-	-	-	660	72	3
Cu	0.54	0.70	3	-	-	-	0.54	0.20	3
Fe	3.63	0.46	3	-	-	-	3.63	0.46	3
Mn	6.73	0.64	3	-	-	-	6.73	0.64	3
Zn	0.53	0.10	3	-	-	-	0.53	0.10	3

TABLE # 3

Brine Parameter	*ERDA 6.8+6.9 (Flow test 2+3) Laboratory			ERDA 6.8+6.9 (Flow test 2+3) Field			ERDA 6.8+6.9 (Flow test 2+3) Field + lab		
	$\bar{x}$	s	n	$\bar{x}$	s	n	$\bar{x}$	s	n
pH	6.42	0.13	10	6.17	0.08	37	6.26	0.15	57
spec. cond.	490,000	34,300	10	472,844	31,114	36	479,686	32,507	56
TDS	330,000	9,900	10	-	-	-	330,000	9,900	10
Ba	0.76	0.76	10	-	-	-	0.76	0.76	10
Ca	490	15	10	-	-	-	490	15	10
Li	240	19	10	-	-	-	240	19	10
Mg	450	85	10	-	-	-	450	85	10
K	3,800	456	10	-	-	-	3,800	456	10
Na	112,000	3,360	10	-	-	-	112,000	3,360	10
Sr	18	2.16	10	-	-	-	18	2.16	10
HCO_3	2,600	52	10	2,578	138	19	2,599	102	39
Br	880	79	10	-	-	-	880	79	10
Cl	170,000	10,200	10	183,700	7,840	19	178,084	13,379	39
F	1.7	0.10	10	-	-	-	1.7	0.10	10
SO_4	16,000	1,120	10	19,463	3,417	19	17,595	3,031	39
$NH_3(N)$	870	17	10	-	-	-	870	17	10
$NO_3(N)$	620	93	10	-	-	-	620	93	10
$PO_4(P)$	0.37	0.07	10	-	-	-	0.37	0.07	10
Al	2.4	1.3	10	-	-	-	2.4	1.3	10
B	680	102	10	-	-	-	680	102	10
Cu	0.49	0.26	10	-	-	-	0.49	0.26	10
Fe	3.6	1.3	10	-	-	-	3.6	1.3	10
Mn	6.9	0.8	10	-	-	-	6.9	0.8	10
Zn	0.55	0.11	10	-	-	-	0.55	0.11	10

TABLE 3

Brine Parameter	ERDA-6.9 (Downhole laboratory) by D'Appolonia			ERDA-6.9 (Downhole Laboratory) by Core			ERDA-6.9 (Downhole Laboratory) D'Appolonia & core		
	$\bar{x}$	s	n	$\bar{x}$	s	n	$\bar{x}$	s	n
pH	7.02	0.14	4	6.7	0.20	4	6.85	0.23	8/4
Cl	180,000	5,400	4	196,300	13,741	4	187,000	13,600	8
SO_4	14,000	420	4	19,980	1,000	4	17,100	3,140	8
HCO_3	1,800	72	4	1,990	60	4	1,870	140	8
TDS	-	-	-	355,700	21,342	4	355,700	21,342	4
Ca	360	32	4	402	12	4	384	30	8
Mg	270	49	4	239	38	4	254	43	8
K	4,800	144	4	3,670	770	4	4,210	780	8
Na	140,000	Ø	4	119,500	1,195	4	129,750	10,980	8
Li	200	6	4	-	-	-	200	6	4
B	740	7.4	4	-	-	-	740	7.4	4
Fe	5.7	1.4	4	-	-	-	5.7	1.4	4

TABLE 3

Brine Parameter	WIPP-12.7 Flow test 1 (Lab)			WIPP-12.7 Flow test 1 (Field)			WIPP-12.7 Flow test 1 (Lab/Field)		
	$\bar{x}$	$\bar{s}$	n	$\bar{x}$	s	n	$\bar{x}$	s	n
pH	7.15	0.02	2	6.81	0.20	7	6.88	0.25	9
spec. cond.	485,000	7,000	2	520,100	52,600	7	517,300	49,900	9
TDS	325,000	7,000	2	-	-	-	325,000	7,000	2
Ba	0.075	0.03	2	-	-	-	0.075	0.03	2
Ca	410	14	2	-	-	-	410	14	2
Li	225	7	2	-	-	-	225	7	2
Mg	1,700	Ø	2	-	-	-	1,700	Ø	2
K	3,100	Ø	2	-	-	-	3,100	Ø	2
Na	115,000	3,500	2	-	-	-	115,000	3,500	2
Sr	14	6	2	-	-	-	14	6	2
HCO_3	2,800	Ø	2	2,840	140	7	2,830	122	9
Br	455	50	2	-	-	-	455	50	2
Cl	165,000	7,000	2	191,100	7,600	7	182,400	14,960	6
F	4.3	Ø	2	-	-	-	4.3	Ø	2
SO_4	16,000	Ø	2	20,400	1,000	7	18,940	2,400	6
$NH_3(N)$	430	Ø	2	-	-	-	430	Ø	2
$NO_3(N)$	570	Ø	2	-	-	-	570	Ø	2
$PO_4(P)$	<.10	Ø	2	-	-	-	<.10	Ø	2
Al	2.3	1.3	2	-	-	-	2.3	1.3	2
B	1,230	150	3	-	-	-	1,230	150	2
Cu	0.63	0.08	2	-	-	-	0.63	0.08	2
Fe	3.15	0.21	2	-	-	-	3.15	0.21	2
Mn	0.35	0.02	2	-	-	-	0.35	0.02	2
Zn	0.47	0.01	2	-	-	-	0.47	0.01	2

TABLE 3

Brine Parameter	WIPP-12.20 Flow Test 3 (Lab)			WIPP-12.20 Flow test 3 (Field)			WIPP-12.20 Flow Test 3 (Lab & Field)		
	x	s	n	x	s	n	x	s	n
pH	7.58	0.08	10	7.09	.07	51	7.17	0.20	61
spec. cond.	680,000	47,600	10	571,400	17,142	51	589,200	46,900	61
TDS	330,000	3,300	10	-	-	-	330,000	3,300	10
Ba	0.3	0.315	10	-	-	-	0.3	0.315	10
Ca	340	24	10	-	-	-	340	24	10
Li	300	18	10	-	-	-	300	18	10
Mg	1,600	48	10	-	-	-	1,600	48	10
K	2,900	232	10	-	-	-	2,900	232	10
Na	140,000	12,600	10	-	-	-	140,000	12,600	10
Sr	20	3.8	10	-	-	-	20	3.8	10
HCO_3	2,660	53	10	2,800	56	47	2,774	86	57
Br	540	59	10	-	-	-	540	59	10
Cl	180,000	12,600	10	181,400	5,442	47	181,390	7,790	57
F	3.1	0.12	10	-	-	-	3.1	0.12	10
SO_4	19,000	950	10	18,800	1,128	47	18,772	1,049	57
NH_3(N)	360	29	10	-	-	-	360	29	10
NO_3(N)	560	263	10	-	-	-	560	263	10
PO_4(P)	<0.3	0.22	10	-	-	-	<0.3	0.22	10
Al	2.9	0.7	10	-	-	-	2.9	0.7	10
B	930	94	10	-	-	-	930	84	10
Cu	0.62	0.21	10	-	-	-	0.62	0.21	10
Fe	2.4	0.4	10	-	-	-	2.4	0.4	10
Mn	0.84	0.13	10	-	-	-	0.84	0.13	10
Zn	0.34	0.05	10	-	-	-	0.34	0.05	10

Brine Parameter	WIPP 12.7 Downhole (Core)			WIPP 12.7 Downhole (D'App.)		
	$\bar{x}$	s	n	$\bar{x}$	s	n
pH	7.3	.07	2	7.76	.06	2
Cl	188,150	15,052	2	180,000	Ø	2
SO_4	20,100	603	2	18,000	Ø	2
HCO_3	2,270	Ø	2	2,400	216	2
TDS	342,000	27,360	2	-	-	-
Ca	310	Ø	2	380	27	2
Mg	1,246	12	2	14,000	Ø	2
K	3,074	9	2	3,200	64	2
Na	119,800	840	2	140,000	7,000	2
Li	-	-	-	210	0	2
B	-	-	-	960	7	2
Fe	-	-	-	6.3	0.6	2
Br	-	-	-	460	9.2	2

Brine Parameter	WIPP-12.8 DST-3020 (lab and D'App.)			Combined Downhole WIPP-12		
	$\bar{x}$	s	n	$\bar{x}$	s	n
pH	7.17	Ø	1	7.44	0.30	5
Cl	160,000			179,000	13,700	5
SO_4	18,000			18,800	1,200	5
HCO_3	2,800			2,450	240	5
TDS	310,000			331,300	25,900	3
Ca	400			356	45	5
Mg	1,600			1,378	146	5
K	3,100			3,110	52	5
Na	112,000			124,320	10,860	5
Li	220			213	6	3
B	1,100			1,003	84	3
Fe	4.5			5.7	1.1	3
Br	380			430	44	3

TABLE 3

Brine Parameter	WIPP-12 Combined Flow Tests		
	$\bar{x}$	s	n
pH	7.14	0.23	71
spec. cond.	579,900	52,400	71
TDS	330,000	4,300	12
Ba	0.62	1.41	12
Ca	350	36	12
Li	290	35	12
Mg	1,630	49	12
K	2,910	240	12
Na	140,000	16,300	12
Sr	19	4.4	12
HCO_3	2,786	90	67
Br	523	64	12
Cl	181,815	8,500	67
F	3.31	0.48	12
SO_4	18,800	1,240	62
NH_3(N)	369	38	12
NO_3(N)	563	238	12
PO_4(P)	0.19	0.21	12
Al	2.8	0.77	12
B	986	164	12
Cu	0.62	0.19	12
Fe	2.54	0.44	12
Mn	0.76	0.22	12
Zn	0.36	0.07	12

TABLE 3

Brine Parameter	WIPP-12.19 Flow test 2 (field)		
	$\bar{x}$	s	$\bar{n}$
pH	7.20	Ø	1
spec. cond.	581,700	Ø	1
HCO_3	2,788	Ø	1
Cl	185,200	Ø	1
SO_4	18,800	Ø	1

TABLE 3

EEG-11 Channell, James K. Calculated Radiation Doses From Radionuclides Brought to the Surface if Future Drilling Intercepts the WIPP Repository and Pressurized Brine, January 1982.

EEG-12 Little, Marshall S. Potential Release Scenario and Radiological Consequence Evaluation of Mineral Resources at WIPP, May 1982.

EEG-13 Spiegler, Peter. Analysis of the Potential Formation of a Breccia Chimney Beneath the WIPP Repository, May 1982.

EEG-14 Zand, Siavosh M. Dissolution of Evaporites and Its Possible Impact on the Integrity of the Waste Isolation Pilot Plant (WIPP) Repository (Draft).

EEG-15 Bard, Stephen T. Estimated Radiation Doses Resulting if an Exploratory Borehole Penetrates a Pressurized Brine Reservoir Assumed to Exist Below the WIPP Repository Horizon - A Single Hole Scenario, February 1982.

EEG-16 Radionuclide Release, Transport and Consequence Modeling for WIPP. A Report of a Workshop Held on September 16-17, 1981, February 1982.

EEG-17 Spiegler, Peter. Hydrologic Analyses of Two Brine Encounters in the Vicinity of the Waste Isolation Pilot Plant (WIPP) Site, December 1982.

EEG-18 Spiegler, Peter and Dave Updegraff. Origin of the Brines Near WIPP from the Drill Holes ERDA-6 and WIPP-12 Based on Stable Isotope Concentrations of Hydrogen and Oxygen, March 1983.

EEG-19 Channell, James K. Review Comments on Environmental Analysis Cost Reduction Proposals (WIPP/DOE-136) July 1982, November 1982.

EEG-20 Baca, Thomas E. An Evaluation of the Non-radiological Environmental Problems Relating to the WIPP, February 1983.

EEG-21 Faith, Stuart, Peter Spiegler, Kenneth R. Rehfeldt. The Geochemistry of Two Pressurized Brines From the Castile Formation in the Vicinity of the Waste Isolation Pilot Plant (WIPP) Site, April 1983.